Declaration of Financial Disclosure

Hideo Takasu is an employee of Dainippon Sumitomo Pharma Co., Ltd.

Acknowledgements

The Authors are grateful to Drs K. Imai and K. Itoh for kindly providing cell lines, and to Dr. T. Kitamura for kindly providing a retrovirus system. This work was supported by Grants-in-Aid for Scientific Research from the Ministry of Education, Culture, Sports, Science and Technology of Japan (grant no. 16209013, 17016061 and 15659097) for Practical Application Research from the Japan Science and Technology Agency, and for Cancer Research (15-17 and 19-14) from the Ministry of Health, Labor and Welfare of Japan, Ono Cancer Research Fund (to N. S.) and Takeda Science Foundation (to Y. H.). This work was supported in part by the National Cancer Center Research and Development Fund (23-A-44).

References

1 Fearon ER and Vogelstein B: A genetic model for colorectal tumorigenesis. Cell *61*: 759-767, 1990.

2 Hanahan D and Weinberg RA: Hallmarks of cancer: the next generation. Cell *144*: 646-674, 2011.

3 Rogalski TM, Mullen GP, Gilbert MM, Williams BD and Moerman DG: The unc-112 gene in *Caenorhabditis elegans* encodes a novel component of cell-matrix adhesion structures required for integrin localization in the muscle cell membrane. J Cell Biol *150*: 253-264, 2000.

4 Weinstein EJ, Bourner M, Head R, Zakeri H, Bauer C and Mazzarella R: URP1: a member of a novel family of PH and FERM domain-containing membrane-associated proteins is significantly overexpressed in lung and colon carcinomas. Biochim Biophys Acta *1637*: 207-216, 2003.

5 Gozgit JM, Pentecost BT, Marconi SA, Otis CN, Wu C and Arcaro KF: Use of an aggressive MCF-7 cell line variant, TMX2-28, to study cell invasion in breast cancer. Mol Cancer Res *4*: 905-913, 2006.

6 Sin S, Bonin F, Petit V, Meseure D, Lallemand F, Bieche I, Bellahcene A, Castronovo V, de Wever O, Gespach C, Lidereau R and Driouch K: Role of the focal adhesion protein kindlin-1 in breast cancer growth and lung metastasis. J Natl Cancer Inst *103*: 1323-1337, 2011.

7 Morita S, Kojima T and Kitamura T: Plat-E: An efficient and stable system for transient packaging of retroviruses. Gene Ther *7*: 1063-1066, 2000.

8 Inoda S, Hirohashi Y, Torigoe T, Nakatsugawa M, Kiriyama K, Nakazawa E, Harada K, Takasu H, Tamura Y, Kamiguchi K, Asanuma H, Tsuruma T, Terui T, Ishitani K, Ohmura T, Wang Q, Greene MI, Hasegawa T, Hirata K and Sato N: Cep55/c10orf3, a tumor antigen derived from a centrosome residing protein in breast carcinoma. J Immunother *32*: 474-485, 2009.

9 Landemaine T, Jackson A, Bellahcene A, Rucci N, Sin S, Abad BM, Sierra A, Boudinet A, Guinebretiere JM, Ricevuto E, Nogues C, Briffod M, Bieche I, Cherel P, Garcia T, Castronovo V, Teti A, Lidereau R and Driouch K: A six-gene signature predicting breast cancer lung metastasis. Cancer Res *68*: 6092-6099, 2008.

10 Siegel DH, Ashton GH, Penagos HG, Lee JV, Feiler HS, Wilhelmsen KC, South AP, Smith FJ, Prescott AR, Wessagowit V, Oyama N, Akiyama M, Al Aboud D, Al Aboud K, Al Githami A, Al Hawsawi K, Al Ismaily A, Al-Suwaid R, Atherton DJ, Caputo R, Fine JD, Frieden IJ, Fuchs E, Haber RM, Harada T, Kitajima Y, Mallory SB, Ogawa H, Sahin S, Shimizu H, Suga Y, Tadini G, Tsuchiya K, Wiebe CB, Wojnarowska F, Zaghloul AB, Hamada T, Mallipeddi R, Eady RA, McLean WH, McGrath JA and Epstein EH Loss of kindlin-1, a human homolog of the *Caenorhabditis elegans* actin-extracellular-matrix linker protein unc-112, causes Kindler syndrome. Am J Hum Genet *73*: 174-187, 2003.

11 Ashton GH, McLean WH, South AP, Oyama N, Smith FJ, Al-Suwaid R, Al-Ismaily A, Atherton DJ, Harwood CA, Leigh IM, Moss C, Didona B, Zambruno G, Patrizi A, Eady RA and McGrath JA: Recurrent mutations in kindlin-1, a novel keratinocyte focal contact protein, in the autosomal recessive skin fragility and photosensitivity disorder, Kindler syndrome. J Invest Dermatol *122*: 78-83, 2004.

12 Has C, Castiglia D, del Rio M, Diez MG, Piccinni E, Kiritsi D, Kohlhase J, Itin P, Martin L, Fischer J, Zambruno G and Bruckner-Tuderman L: Kindler syndrome: Extension of FERMT1 mutational spectrum and natural history. Hum Mutat *32*: 1204-1212, 2011.

13 Malinin NL, Zhang L, Choi J, Ciocea A, Razorenova O, Ma YQ, Podrez EA, Tosi M, Lennon DP, Caplan AI, Shurin SB, Plow EF and Byzova TV: A point mutation in *KINDLIN3* ablates activation of three integrin subfamilies in humans. Nat Med *15*: 313-318, 2009.

14 Svensson L, Howarth K, McDowall A, Patzak I, Evans R, Ussar S, Moser M, Metin A, Fried M, Tomlinson I and Hogg N: Leukocyte adhesion deficiency-III is caused by mutations in *KINDLIN3* affecting integrin activation. Nat Med *15*: 306-312, 2009.

15 He Y, Esser P, Heinemann A, Bruckner-Tuderman L and Has C: Kindlin-1 and -2 have overlapping functions in epithelial cells implications for phenotype modification. Am J Pathol *178*: 975-982, 2011.

16 Bandyopadhyay A, Rothschild G, Kim S, Calderwood DA and Raghavan S: Functional differences between kindlin-1 and kindlin-2 in keratinocytes. J Cell Sci *125*: 2172-2184, 2012.

Received October 29, 2012
Revised November 12, 2012
Accepted November 13, 2012

釣田　義一郎
（東京大学）

OPEN ACCESS Freely available online

PLOS ONE

Overexpression of Cohesion Establishment Factor DSCC1 through E2F in Colorectal Cancer

Kiyoshi Yamaguchi[1]*, Rui Yamaguchi[2], Norihiko Takahashi[1], Tsuneo Ikenoue[1], Tomoaki Fujii[1], Masaru Shinozaki[3], Giichiro Tsurita[3], Keisuke Hata[3], Atsushi Niida[4], Seiya Imoto[4], Satoru Miyano[2,4], Yusuke Nakamura[5], Yoichi Furukawa[1]

1 Division of Clinical Genome Research, Advanced Clinical Research Center, Institute of Medical Science, The University of Tokyo, Tokyo, Japan, **2** Laboratory of Sequence Analysis, Human Genome Center, Institute of Medical Science, The University of Tokyo, Tokyo, Japan, **3** Department of Surgery, Research Hospital, Institute of Medical Science, The University of Tokyo, Tokyo, Japan, **4** Laboratory of DNA Information Analysis, Human Genome Center, Institute of Medical Science, The University of Tokyo, Tokyo, Japan, **5** Laboratory of Molecular Medicine, Human Genome Center, Institute of Medical Science, The University of Tokyo, Tokyo, Japan

Abstract

Ctf18-replication factor C complex including Dscc1 (DNA replication and sister chromatid cohesion 1) is implicated in sister chromatid cohesion, DNA replication, and genome stability in *S. cerevisiae* and *C. elegans*. We previously performed gene expression profiling in primary colorectal cancer cells in order to identify novel molecular targets for the treatment of colorectal cancer. A feature of the cancer-associated transcriptional signature revealed from this effort is the elevated expression of the proto-oncogene *DSCC1*. Here, we have interrogated the molecular basis for deviant expression of human DSCC1 in colorectal cancer and its ability to promote survival of cancer cells. Quantitative PCR and immunohistochemical analyses corroborated that the expression level of DSCC1 is elevated in 60–70% of colorectal tumors compared to their matched noncancerous colonic mucosa. An *in silico* evaluation of the presumptive *DSCC1* promoter region for consensus DNA transcriptional regulatory elements revealed a potential role for the E2F family of DNA-binding proteins in controlling DSCC1 expression. RNAi-mediated reduction of E2F1 reduced expression of DSCC1 in colorectal cancer cells. Gain- and loss-of-function experiments demonstrated that DSCC1 is involved in the viability of cancer cells in response to genotoxic stimuli. We reveal that E2F-dependent expression of DSCC1 confers anti-apoptotic properties in colorectal cancer cells, and that its suppression may be a useful option for the treatment of colorectal cancer.

Citation: Yamaguchi K, Yamaguchi R, Takahashi N, Ikenoue T, Fujii T, et al. (2014) Overexpression of Cohesion Establishment Factor DSCC1 through E2F in Colorectal Cancer. PLoS ONE 9(1): e85750. doi:10.1371/journal.pone.0085750

Editor: Srikumar P. Chellappan, H. Lee Moffitt Cancer Center & Research Institute, United States of America

Received October 28, 2013; **Accepted** November 30, 2013; **Published** January 17, 2014

Funding: This work was supported in part by Grant-in-Aid for Young Scientists (#23790126), MEXT/JSPS, Japan to K. Yamaguchi, and Global COE Program "Center of education and research for the advanced genome-based medicine for personalized medicine and the control of worldwide infectious diseases", MEXT/Japan Society for the Promotion of Science, Japan to Y. Furukawa. The funders had no role in study design, data collection and analysis, decision to publish, or preparation of the manuscript.

Competing Interests: The authors have declared that no competing interests exist.

* E-mail: kiyamagu@ims.u-tokyo.ac.jp

Introduction

Colorectal cancer (CRC) is one of the most frequent human neoplasms in the world. In CRC cells, disruption of systems governing genetic or epigenetic integrity renders different features such as chromosomal instability (CIN), microsatellite instability (MSI), and CpG island methylator phenotype (CIMP). A great majority of colorectal tumors exhibit CIN that includes gross genetic changes such as deletions, amplifications, inversions, rearrangements, gain or loss of whole or large portions of chromosomes, and translocations [1]. An earlier study identified somatic mutations in five genes including *MRE11*, *ZW10*, *ZWILCH*, *ROD*, and *DING*, among 100 human CIN-candidate genes that shared similarity with yeast or fly "instability" genes [2]. Their data suggested that at least one of three functions including double-strand break repair, kinetochore function, and chromatid segregation, is impaired in CIN tumors by somatic mutation. Another study searched for mutations of 102 human homologues of yeast CIN genes in 132 colorectal cancers. Consequently, they identified a total of 11 mutations in five genes that included four associated with sister chromatid cohesion (*SMC1L1*, *CSPG6*, *NIPBL*, and *STAG3*, the homologues of yeast *SMC1*, *SMC3*, *SCC2*, and *SCC3*, respectively) [3]. Since sister chromatid cohesion is indispensable for cellular processes such as chromosome segregation, homologous recombinational repair, and regulation of transcription [4], genetic alterations in the components and regulators should play a crucial role in the CIN of colorectal tumors.

We previously performed gene expression profile analysis in CRC [5], and identified that DNA replication and sister chromatid cohesion 1 (*DSCC1*, also known as *DCC1*) was frequently elevated in colorectal tumors compared with non-cancerous colonic mucosa. Dcc1p, a homolog of DSCC1, was first identified as a member of alterative replication factor C (RFC) complex in the yeast, and physically associates with Ctf8p and Ctf18p [4]. Deletion of the component, Ctf18p, Ctf8p, or Dcc1p, resulted in severe sister chromatid cohesion defects, and increased sensitivity to microtubule depolymerizing drugs, suggesting that these components are essential for maintenance of chromatin integrity [4]. Although Dcc1p was not essential for the viability of yeast, deletion of Dcc1p led to synthetic lethality in combination

with mutation of other sister chromatid cohesion proteins [6]. In addition to the implication in sister chromatid cohesion, the CTF18-DSCC1-CTF8-RFC complex plays a crucial role in DNA replication through the interaction with single-stranded and primed DNA as a loader of proliferating cell nuclear antigen [7]. Furthermore, genetic network analysis of functionally related genes in the yeast suggested that the components of CTF18-DSCC1-CTF8-RFC complex interact with the MAD/BUB spindle checkpoint pathway, the RAD51 DNA repair pathway for double-strand breaks, the RAD9 DNA damage checkpoint, and the TOF1/MRC DNA replication checkpoint pathway [8,9]. The finding that mutation in CTF18-RFC increased triplet repeat instability corroborated the role of this complex in the DNA-replication checkpoint [10]. These data indicated that DSCC1 plays an important role in replication, spindle checkpoint and DNA repair, which prompted us to investigate whether deregulated expression of DSCC1 is involved in human colorectal tumorigenesis.

Here, we show for the first time that DSCC1 is frequently up-regulated in CRC at least in part through the enhanced transcriptional activation by E2F. We also reveal that elevated expression of DSCC1 confers chemoresistance in CRC cells by providing tumor cells with anti-apoptotic properties. These findings will contribute to a better understanding of CRC, and serve as a starting point for the development of novel strategies for diagnosis and treatment of CRC.

Materials and Methods

Ethics statement

This project was approved by the ethical committee of Institute of Medical Science, the University of Tokyo (IMSUT-IRB, 21-14-0806). Written informed consent was obtained from all patients in this study. All colorectal cancer tissues and corresponding non-cancerous tissues were obtained from surgical specimens of patients who underwent surgery.

Cell culture

Human CRC cell lines HCT116, HCT-15, SW480, DLD-1, LoVo, Caco-2, LS174T, HT-29, and RKO were purchased from the American Type Culture Collection (Manassas, VA). All cells were grown in appropriate media supplemented with FBS (Life Technologies, Carlsbad, CA) and antibiotic/antimycotic solution (Sigma, St. Louis, MO).

Preparation of plasmids expressing DSCC1 and E2Fs

The entire coding region of *DSCC1* cDNA (GenBank accession No. NM_024094) was amplified by RT-PCR using a set of primers; forward primer: 5′-CCGGAATTCATGAAGAG-GACCCGCGAC-3′ and reverse primer: 5′-CGGCTCGAGA-GAAATGGGTCTTCTCGAATTAT-3′ (underlined nucleotides indicate the recognition sites of restriction enzymes). The PCR products were cloned into the *Eco*RI and *Xho*I sites of pcDNA3.1/myc-His. We additionally generated plasmids expressing HA-tagged DSCC1 (pCAGGS-DSCC1). The constructs pcDNA3-HA-E2Fs were kindly provided by Dr. J. R. Nevins (Duke University, Durham, NC).

Quantitative PCR and gene copy number analysis

Real-time PCR was performed using the LightCycler 480 system (Roche Diagnostics, Indianapolis, IN). Genomic DNAs were extracted from CRC cell lines for copy number analysis. Quantitative PCR was performed on ABI PRISM 7900HT Sequence Detection System, using FAM-labeled probes (5′-TCAGGTTTCCTACCTTCCGGCTGCTT-3′) and a set of primers (forward: 5′-GGCGCGCTTTCAAACG-3′, reverse: 5′-GCGGGCAAGAAAGAAGTTCC-3′) for *DSCC1*, and TaqMan Copy Number Reference Assays RNase P as a quantitative control (Life Technologies). The copy number of *DSCC1* in the cancer cells was calculated in comparison with genomic DNA from healthy volunteers using CopyCaller Software.

Subcellular fractionation and immunoblotting

Cells were lysed in radioimmunoprecipitation assay buffer (50 mM Tris-HCl, pH 8.0, 150 mM NaCl, 0.5% sodium deoxycholate, 1% Nonidet P-40, 0.1% SDS) supplemented with a Protease Inhibitor Cocktail Set III (Calbiochem, San Diego, CA). Nuclear extracts were prepared using Nuclear Extract Kit (Active Motif, Carlsbad, CA). Proteins were separated by SDS-PAGE and immunoblot analysis was performed using the indicated antibodies. Horseradish peroxidase-conjugated goat anti-mouse or anti-rabbit IgG (GE Healthcare, Buckinghamshire, UK) served as the secondary antibody for the ECL Detection System (GE Healthcare).

Immunostaining

Primary antibodies used for immunohistochemical and immunocytochemical staining were anti-DSCC1 (B01P, Abnova, Taipei, Taiwan) and anti-Myc (Sigma). The specificity of DSCC1 antibody was confirmed by the blocking with DSCC1 recombinant protein (data not shown). These experiments were performed as described previously [11].

Induction of apoptosis and flow cytometry

To study the induction of apoptosis, cells were treated with camptothecin (Wako, Osaka, Japan), doxorubicin (LC Laboratories, Woburn, MA), MG132 (Merck Millipore, Darmstadt, Germany), or exposed to γ-irradiation (Gammacell 40, Atomic Energy of Canada, Ontario, Canada). Expression of cleaved poly (ADP-ribose) polymerase (PARP) and cleaved caspase-3 was detected by western blot analysis using anti-cleaved PARP (9541) and anti-caspase-3 antibodies (9662), respectively (Cell Signaling Technology, Danvers, MA). Assessment of apoptosis was also performed by annexin V and PI double-staining using Alexa Fluor 488 Annexin V/Dead Cell Apoptosis Kit (Life Technologies). Briefly, cultured cells were treated with vehicle or camptothecin for 24 h. The cells were stained with Annexin V and PI, and subsequently analyzed on a FACSCalibur (Becton Dickinson, Franklin Lakes, NJ) using FlowJo software (Tree Star, Ashland, OR).

Cell viability assay

Plasmids expressing short hairpin RNA (shRNA) using U6 promoter (psiU6BX3.0) were prepared as described previously [12]. Plasmids expressing DSCC1 shRNA (psiU6-shDSCC1) were constructed by cloning double-stranded oligonucleotides into the *Bbs*I sites of the psiU6BX3.0 vector. Two target sequences, 5′-GUGGACAGAAGAAGAUAUU-3′ (shDSCC1#1) and 5′-GCAAACCAUAGGUGCAUUA-3′ (shDSCC1#2), were used for DSCC1 shRNAs. As negative controls, we prepared a plasmid targeting enhanced green fluorescent protein (psiU6-shEGFP) and those targeting scrambled sequences of shDSCC1#1 (5′-AAAUUGCGAAGGUGAUGAA-3′; psiU6-shDSCC1#1scr) or shDSCC1#2 (5′-AACACGUUAAUAACCGGUG-3′; psiU6-shDSCC1#2scr). Cell viability assays were carried out as described previously using HCT116, SW480, and RKO cells transfected with plasmids expressing shEGFP, shDSCC1, or

scramble shDSCC1 [11]. To investigate the effect of DSCC1 overexpression on cell proliferation, we transfected SW480 and HCT116 cells with pCAGGS-DSCC1 and established two or three clones stably expressing exogenous DSCC1. Control SW480 and HCT116 cells transfected with empty vector were also established as mock cells.

Promoter reporter assays and site-directed mutagenesis

Luciferase reporter plasmids containing the *DSCC1* promoter were prepared by cloning the 5′-flanking region of *DSCC1* into the *Mlu*I and *Bgl*II restriction enzyme sites of pGL3-Basic vector (Promega, Madison, WI). A DNA fragment of approximately 1.0-kb in the 5′-flanking region of *DSCC1* was amplified by PCR using genomic DNA from healthy volunteers and a set of primers (forward: 5′-CGACGCGTATGTCTGCTCAGATCCTTT-GAAT-3′, reverse: 5′-GAAGATCTCGCCGGGTCTAG-GAGTCC-3′). Mutant plasmids containing substitutions in putative E2F binding sites of the *DSCC1* promoter were generated by site-directed mutagenesis using the QuikChange II XL Site-Directed Mutagenesis Kit (Agilent Technologies, Santa Clara, CA). Cells seeded into 6-well plates were transfected with the reporter plasmids together with pRL-TK (Promega) using FuGENE 6 reagent. Cells were harvested 24 hours after transfection, and reporter activities were measured by dual luciferase system (TOYO B-Net, Tokyo, Japan). For the knock-down of E2F1 expression, synthetic E2F1 siRNA was purchased from Sigma (sense: 5′-GGGAGAAGUCACGCUAUGA-3′, anti-sense: 5′-AUAGCGUGACUUCUCCCCC-3′).

Chromatin immunoprecipitation assay

To investigate the interaction of E2F1 with the *DSCC1* promoter region, a chromatin immunoprecipitation (ChIP) assay was performed according to the Agilent Mammalian ChIP protocol with slight modifications. HCT116 cells were cross-linked with 1% formaldehyde for 10 min at room temperature and quenched with 0.4 M glycine. Chromatin extracts were sheared by micrococcal nuclease digestion, and subsequently protein-DNA complexes were immunoprecipitated with 3 μg of anti-E2F1 polyclonal antibody (C-20, Santa Cruz Biotechnology, Santa Cruz, CA) bound to anti-rabbit IgG-coated Dynabeads (Life Technologies). Non-immune rabbit IgG (Santa Cruz Biotechnology) was used as a negative control. The precipitated DNAs were subjected to quantitative PCR analysis with a primer set (forward (−26) 5′-CCGGAAACACGCCCATGGC-3′ and reverse (+127) 5′-GGGTCCTCTTCATCGCAGC-3′) to amplify the *DSCC1* promoter region. Specificity of the assay was determined by the amplification of a distal upstream region in the *DSCC1* promoter with the following primers: forward (−1279) 5′-AGTTGTAGG-GAATGTTTTCCCATT-3′ and reverse (−1111) 5′-GATTGGTTCATGTGACCTACTTC-3′. In addition, the amplifications of cell division cycle 2 (*CDC2*) promoter and glyceraldehyde-3-phosphate dehydrogenase (*GAPDH*) promoter were used for positive and negative controls, respectively (primers: *CDC2* forward 5′-CGCCCTTTCCTCTTTCTTTC-3′, *CDC2* reverse 5′-ATCGGGTAGCCCGTAGACTT-3′, *GAPDH* forward 5′-TACTAGCGGTTTTACGGGCG-3′, *GAPDH* reverse 5′-TCGAACAGGAGGAGCAGAGAGCGA-3′).

Results

Expression of DSCC1 is frequently elevated in CRC

In order to identify novel target molecules for the treatment and/or diagnostic biomarkers of CRC, we previously performed expression profile analysis of colorectal tumors and their matched normal colorectal tissues by cDNA microarray [5]. Among the genes deregulated in colorectal tumors, expression of DNA replication and sister chromatid cohesion 1 (*DSCC1*) was increased more than two-fold in 5 of 7 colorectal cancers compared with corresponding non-cancerous colon mucosa (Figure 1A). Subsequent real-time PCR analysis using an additional 20 CRC tissues and the corresponding non-cancerous mucosa revealed that *DSCC1* expression was elevated more than two-fold in 12 of the 20 tumors (Figure 1A). An immunohistochemical staining showed accumulated DSCC1 protein in 29 of 40 CRC tissues compared with corresponding adjacent non-cancerous colonic mucosa (Figure 1B). Although we searched for correlations between its expression and clinicopathological factors including age and sex of the patients, location, size, and histological data of the tumors such as depth of invasion, lymph node involvement, and vascular or lymphatic vessel invasion, none of the factors was significantly associated with DSCC1 expression (Table S1). Additionally, western blot analysis using CRC cell lines revealed that DSCC1 was abundantly expressed in HCT116, HT-29, and DLD-1 cells, and that it was expressed at low levels in SW480, SW620, and Caco-2 cells (Figure 1C). Although we compared stability of DSCC1 protein in HCT116 (DSCC1-high) and SW480 (DSCC1-low) cells by cycloheximide chase assay, DSCC1 was relatively stable in both HCT116 and SW480 cells. Treatment with MG132, a proteasome inhibitor also did not enhance DSCC1 expression (Figure S1A). These data suggested that protein stability is not likely to play a major role in the elevated expression of DSCC1 in cancer cells.

Immunohistochemical analysis unexpectedly depicted accumulated DSCC1 in the cytoplasm and nucleus of DSCC1-positive cancer cells (Figure 1B), although Dscc1 was reported to play a role in the establishment of cohesion during DNA replication in the yeast. To elucidate its subcellular localization, we carried out immunocytochemical staining of endogenous DSCC1 in HCT116 cells. Consistent with the immunohistochemical staining of cancer tissues, DSCC1 protein was localized in both cytoplasm and nucleus (Figure 1D and S1B). Furthermore, western blot analysis using cytoplasmic and nuclear fractions extracted from HCT116, RKO, and DLD-1 cells (Figure 1E) and cells expressing Myc-tagged DSCC1 confirmed its subcellular localization in the cytoplasm as well as the nucleus (Figure S1C and S1D).

Copy number analysis of *DSCC1*

To address whether gene amplification is involved in the DSCC1 overexpression, we conducted copy number analysis by quantitative PCR using RNase P as a control. Compared with peripheral leukocytes from healthy volunteers, the copy number of *DSCC1* was not increased in any CRC cell lines tested (Figure 1F). It is worth noting that a decrease in copy number was observed in HT-29 cells that abundantly expressed DSCC1 (Figure 1C). We further analyzed copy number alteration of *DSCC1* in colon and rectum adenocarcinoma (The Cancer Genome Atlas Colorectal Cancer project) using the cBioPortal database (http://www.cbioportal.org/public-portal/). As a result, putative copy number changes were found in 7 of 257 colorectal adenocarcinomas (2.7%), suggesting that amplification of *DSCC1* does not play a major role in the enhanced DSCC1 expression.

Regulation of *DSCC1* promoter activity

To resolve the mechanism of elevated DSCC1 expression in CRC, we investigated the promoter activity of *DSCC1* in HCT116 cells. Reporter assay using plasmids containing a 5′-flanking region of *DSCC1* (pDSCC1-1023/+109) showed that this region has a substantial promoter activity (data not shown). In the region,

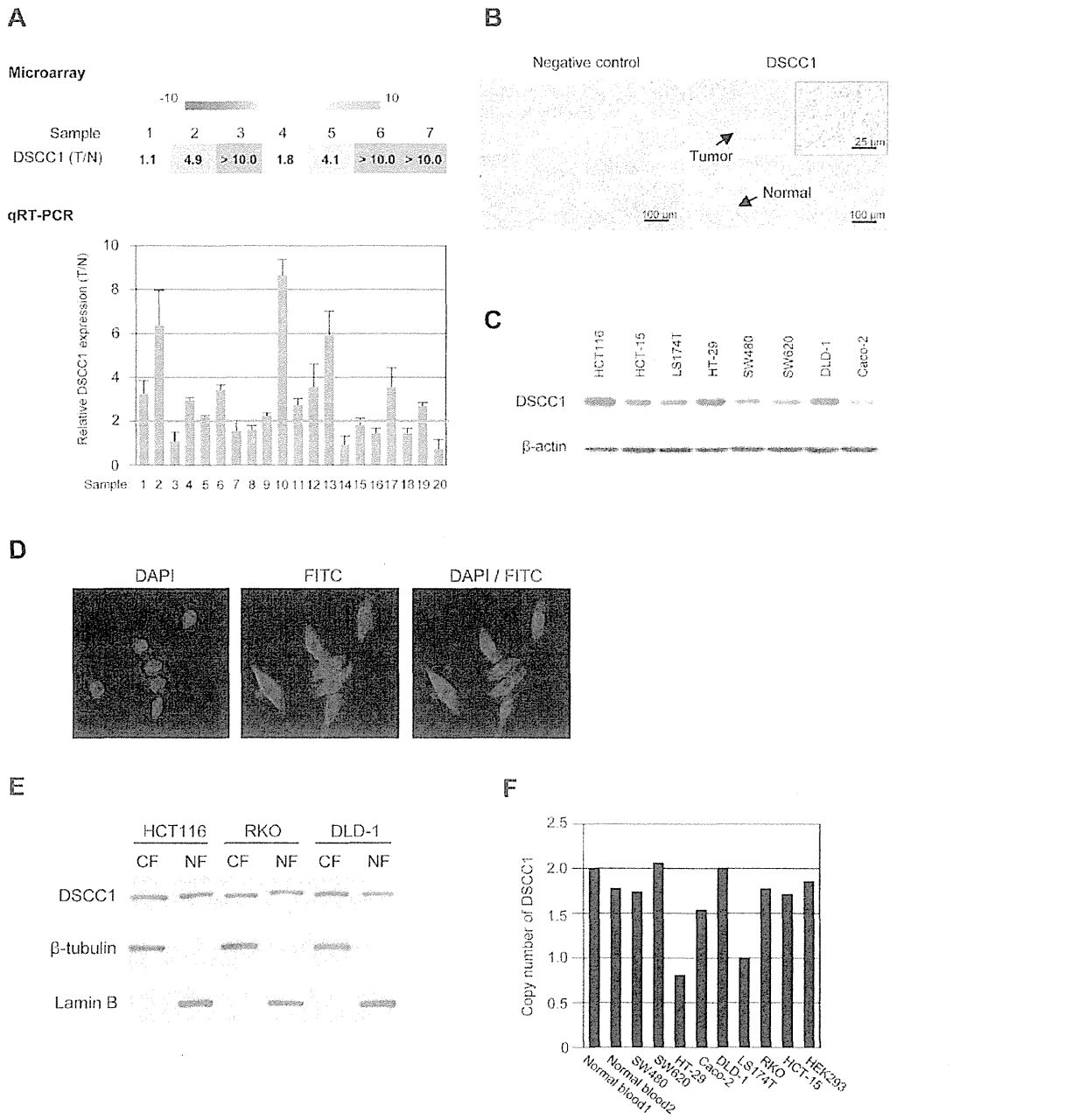

Figure 1. Expression of DSCC1 in colorectal tumors. (A) Relative expression ratios of *DSCC1* in seven colorectal cancer tissues to their corresponding normal tissues in our microarray data (upper panel). Relative expression levels of *DSCC1* in an additional 20 colorectal tumors and the corresponding non-cancerous mucosa was analyzed by quantitative PCR (lower panel). Quantity of *DSCC1* was normalized to *HPRT1* expression. Y axis indicates the ratio of mean of *DSCC1* expression in tumor to that in their corresponding normal tissue. The data represents mean ± SD from triplicate experiments. (B) Representative image of immunohistochemical staining of DSCC1 in a human colon cancer tissue containing cancer cells and adjacent normal mucosa. (C) Expression of DSCC1 in CRC cell lines was detected by western blotting using anti-DSCC1 antibody. (D) HCT116 cells were probed with anti-DSCC1 antibody followed by FITC-conjugated anti-mouse IgG secondary antibody (green). Nuclei were counter-stained with DAPI (blue). (E) HCT116, RKO, and DLD-1 cells were separated into the cytoplasmic (CF) and nuclear fractions (NF), and the cytoplasmic and nuclear proteins were subjected to SDS-PAGE followed by western blotting. Purity of the fractions was determined by the presence of β-tubulin (cytoplasmic marker) and lamin B (nuclear marker). (F) Copy number analysis of *DSCC1* in eight CRC cell lines and HEK293 cells. Relative copy number of *DSCC1* gene was determined by quantitative PCR using *RPPH1* as an endogenous reference. The copy number was calculated by dividing their PCR products by those of peripheral leukocytes from healthy volunteers, and subsequently multiplying by 2.
doi:10.1371/journal.pone.0085750.g001

we identified a putative E2F-binding motif, EBS1 (−3/+5; 5′-CTTGGCGC-3′) using the JASPAR (http://jaspar.genereg.net/) and TFSEARCH databases (http://www.cbrc.jp/research/db/TFSEARCH.html) (Figure 2A). This putative binding site shared high similarity with the consensus motif for E2F, TTTSSCGC with S = G or C. Since E2F transcription factors are frequently deregulated in a variety of tumors, we tested the effect of E2Fs on the *DSCC1* promoter activity. Although E2F1, E2F2, E2F3, and E2F4 increased the promoter activity, E2F6 did not change the activity. E2F1, which showed the strongest induction among the four members, augmented the activity in a dose-dependent fashion (Figure 2B and S2A). This enhancement was also observed in other cell lines including LoVo, HeLa, and HEK293 (data not shown). To examine the possible involvement of EBS1 in the enhancement, we measured reporter activity using the constructs pDSCC1-10/+109 and +10/+109 in the presence or absence of E2F1 (Figure 2C). Basal reporter activities of these reporter plasmids were not significantly different in the absence of E2F1 plasmids. Deletion of EBS1 (pDSCC1+10/+109) dramatically decreased E2F1-induced reporter activity (from 20.4-fold to 3.2-fold). Unexpectedly, enhancement of reporter activity by E2F1 was still observed in +10/+109. Further deletion up to +70 of the promoter (pDSCC1+70/+109) completely diminished E2F1-induced reporter activity (Figure 2C). In agreement with this result, we found two additional presumptive EBSs, EBS2 (+31/+38; 5′-CTTCCGGC-3′) and EBS3 (+57/+64; 5′-TTGCCCGC-3′) in the region between +10 and +70. To address responsibilities of EBS1, EBS2, and EBS3 for the induction, we prepared four mutant reporter constructs (Figure 2D) by substituting the GC-rich segment in E2F consensus motifs, TTTSSCGC (S = C or G) or STTTS, because these core motifs were reportedly crucial for E2F binding [13,14]. Compared with wild type pDSCC1-10/+109 (14.8-fold induction), both types of EBS1-mutant plasmids (pDSCC1-10/+109 mut1, and mut1′) remarkably decreased the reporter activity in response to E2F1 (5.2-fold and 5.8-fold, respectively). Mutations in both EBS1 and EBS2 (pDSCC1-10/+109 mut1+2) further decreased in the E2F1-induced activity (3.7-fold). Mutant reporter plasmid containing substitutions in the three elements (pDSCC1-10/+109 mut1+2+3) almost diminished the enhancement (1.7-fold), suggesting that the three E2F binding motifs are responsible for the regulation of *DSCC1* promoter activity.

Interaction of E2F1 with the *DSCC1* promoter region

To determine whether E2F1 binds to the promoter region of *DSCC1*, we performed quantitative ChIP assay using anti-E2F1 antibody and a set of primers encompassing the three putative E2F-binding elements. The promoter of cell division cycle 2 gene (*CDC2*), a well-known E2F1 target, was enriched 13.4-fold with the immunoprecipitated DNA (Figure S2B). Expectedly, the *DSCC1* promoter region was enriched by up to 15.4-fold in the DNA, suggesting an interaction of the *DSCC1* promoter region with E2F1 (Figure 2E).

To confirm the involvement of E2F1 in regulating DSCC1 expression, we investigated the silencing effect of E2F1 on DSCC1 expression. Real-time PCR and western blot analyses showed that depletion of E2F1 decreased DSCC1 expression (Figure 2F and S2C). RNAi-mediated knockdown of E2F1 activity was confirmed by reporter assay showing significant reduction of the *DSCC1* promoter activity from 10.4 (Ctrl siRNA) to 4.7-fold by E2F1 siRNA in SW480 cells (Figure 2G). These results suggested that *DSCC1* transactivation is, at least in part, regulated by E2F1 in CRC through its interaction with the *DSCC1* promoter region, and that the three EBSs play an important role in the transcriptional activation. To further investigate whether DSCC1 expression is modulated by E2F transcriptional activity, we compared the relative expression of *DSCC1* with *CDK1* (*CDC2*), as readout of E2F transcriptional activity, using two independent data sets (E-MEXP-3715 and GEOD-23878) in the Gene Expression Atlas database (http://www.ebi.ac.uk/gxa/). In the data sets, *DSCC1* and *CDK1* were significantly up-regulated in colorectal tumors compared with normal colonic tissues (Figure 3). Notably, both data sets calculated high values of correlation coefficient (E-MEXP-3715, $r=0.912$ and GEOD-23878, $r=0.864$) between *DSCC1* and *CDK1*, supporting the view that *DSCC1* is another downstream gene regulated by E2F.

Effect of DSCC1 on the proliferation of CRC cells

To address the role of its elevated expression in CRC cells, we investigated whether DSCC1 is involved in the proliferation of cancer cells. We carried out cell viability assay using plasmids expressing both DSCC1 shRNA (shDSCC1#1, or shDSCC1#2) and neomycin resistant gene. Plasmids containing the scrambled sequence of DSCC1 shRNAs (shDSCC1#1scr and shDSCC1#2scr) and plasmid containing EGFP shRNA (shEGFP) served as controls. Transfection with these DSCC1 shRNAs (shDSCC1#1, or shDSCC1#2) reduced the expression of DSCC1, whereas transfection with controls (shEGFP, shDSCC1#1scr and shDSCC1#2scr) had no effect (Figure 4A). HCT116 cells were cultured in media containing appropriate concentration of G418 and the cell viability was measured. We found that the number of viable cells transfected with DSCC1#1 or DSCC1#2 shRNA was significantly decreased compared to those transfected with EGFP, DSCC1#1scr, or DSCC1#2scr shRNA, indicating that DSCC1 plays a role in the viability of cancer cells (Figure 4B). Consistent data was obtained in SW480 and RKO cells (Figure S3A). These results were confirmed in repeated experiments.

In addition, we established SW480 cells that constitutively express exogenous DSCC1, and compared their proliferation with control cells transfected with mock vector (Figure 4C). Consistent with the DSCC1-knockdown data, cells expressing exogenous DSCC1 showed augmented cell proliferation compared to parental SW480 cells or control cells ($p=2.2\times10^{-5}$). Similarly, exogenous DSCC1-expression enhanced the proliferation of HCT116 cells (Figure S3B).

Role of DSCC1 in the induction of apoptosis

Since E2F1 conferred resistance to genotoxic insults [15,16,17], we further investigated whether elevated DSCC1 expression plays a role in the sensitivity of cancer cells to genotoxic stimuli. SW480 cells-expressing exogenous DSCC1 (SW480-DSCC1#1, #3, and #8) were exposed to γ-irradiation, and induction of apoptosis was analyzed by immunoblotting with anti-cleaved PARP antibody. As shown in Figure 5A, quantification of cleaved PARP-specific bands revealed that γ-irradiation led to 3.9, 2.6, and 1.2-fold increase of cleaved PARP in control cells (SW480-Mock#1, #3, and #4, respectively). On the other hand, 1.0, 1.4, and 1.2-fold increase was observed in response to γ-irradiation in SW480-DSCC1#1, #3, and #8 cells, respectively, suggesting that DSCC1 suppressed apoptosis by γ-irradiation. In addition, treatment with camptothecin, an inhibitor of topoisomerase I, induced early apoptotic cells (annexin V-positive and PI-low) by 5.6±2.9% in control cells (Figure 5B), while the treatment increased early apoptotic cells by only 0.7±0.3% in SW480-DSCC1 cells, indicating a significant suppression of apoptosis ($p=0.02$). These data suggested that elevated DSCC1 expression might confer resistance to apoptotic stimuli in cancer cells. In

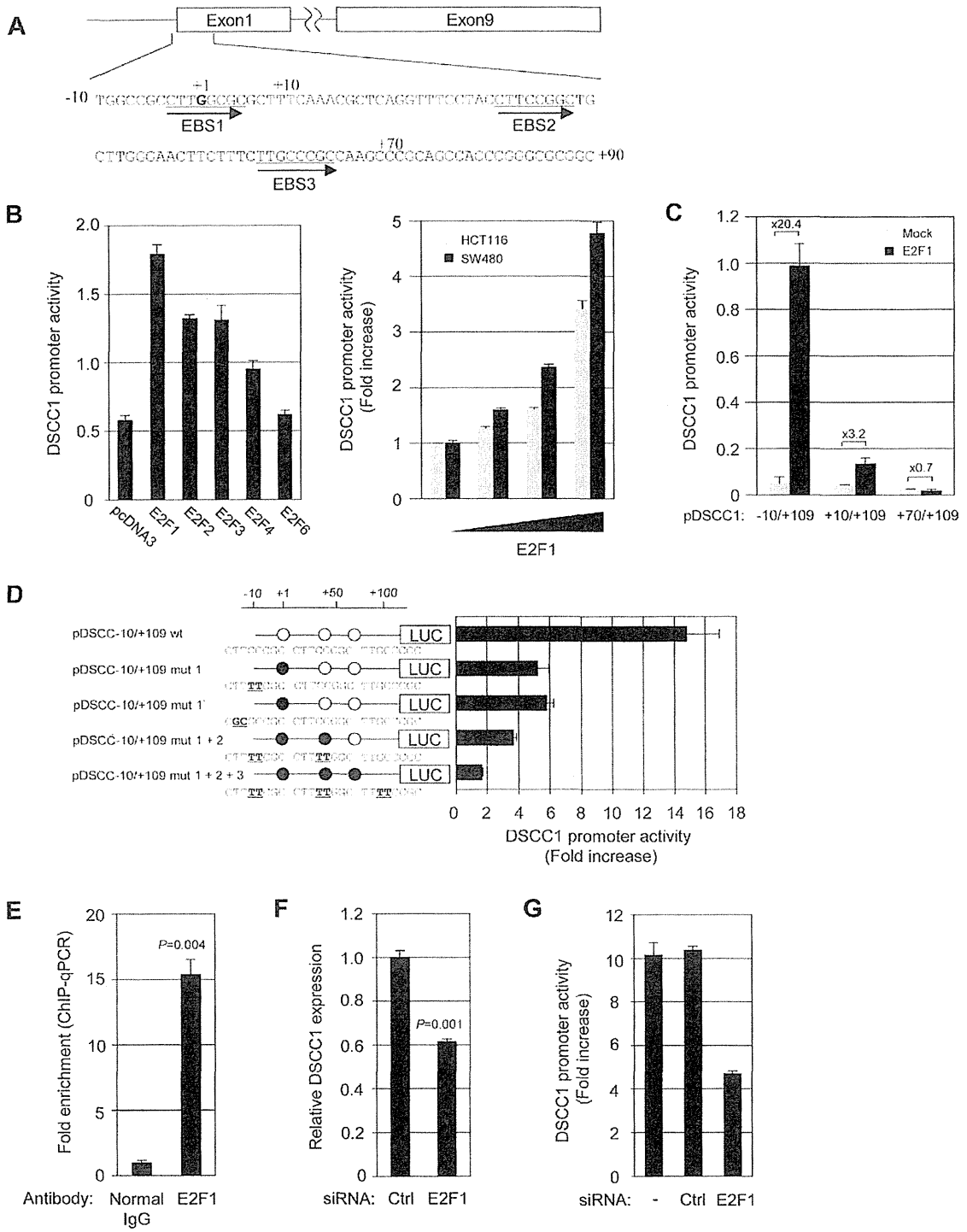

Figure 2. Regulation of *DSCC1* promoter activity by E2F transcription factor. (A) Nucleotide sequence of the −10 to +90 bp region human *DSCC1*. Three putative E2F binding motifs are underlined. (B) pDSCC1-1023/+109 was transiently transfected with pRL-TK and pcDNA3 HA-E2Fs into SW480, or with pRL-TK and pcDNA3 HA-E2F1 (0.01-1 μg) into SW480 and HCT116 cells. (C) pDSCC1-10/+109 or the shorter promoter constructs was transfected with E2F1 or the empty vector into SW480 cells. (D) Site-directed mutation analysis of putative E2F binding sites in the proximal promoter region. pDSCC1-10/+109 or its mutant clones was transfected with E2F1 or the empty vector into SW480 cells. The data represents mean ± SD from three independent experiments. Promoter activity indicates the relative luciferase unit or the fold induction over empty vector transfectant. (E) Chromatin immunoprecipitation was performed using anti-E2F1 antibody. The precipitated DNAs were subjected to the amplification of *DSCC1*

promoter by quantitative PCR. To ascertain the specific binding to the EBS, the amplification of a distal upstream region in the *DSCC1* promoter was used for normalization. A significant difference was determined by t-test. (F) HCT116 cells were transfected with control or E2F1 siRNA (25 nM) for 48 h. *DSCC1* expression was detected by quantitative PCR. A significant difference was determined by t-test. (G) SW480 cells were transfected with control or E2F1 siRNA (25 nM), followed 8 h later by transfection with reporter plasmid (pDSCC1-10/+109) and E2F1 expression vector or the empty vector. After 48 h, luciferase activity was measured. The data represents mean ± SD from three independent experiments.
doi:10.1371/journal.pone.0085750.g002

complete agreement with these results, knockdown of DSCC1 potentiated camptothecin- and γ-irradiation-induced apoptosis in HCT116 cells (Figure 5C and S3C). To address whether DSCC1 expression affects cell death induced by other types of cytotoxic reagents, we treated HCT116 cells with doxorubicin, a DNA intercalator, or MG132, a proteasome inhibitor, and measured the cleavage of PARP and caspase-3, indicators of apoptosis. Suppression of DSCC1 augmented the cleavage of PARP and caspase-3 in response to doxorubicin, whereas knockdown of DSCC1 did not increase the cleavage in response to MG132 (Figure S3D and S3E). Therefore, DSCC1 may be associated with the cell death caused by DNA-damage, but not with the death by other types of cytotoxic insults. Of note, DSCC1 depletion also enhanced induction of apoptosis by γ-irradiation in p53-null HCT116 cells (Figure S3F), suggesting that DSCC1-mediated resistance against apoptosis was independent of p53. These results imply that suppression of DSCC1 may be useful for the treatment and/or chemosensitization of CRC cells.

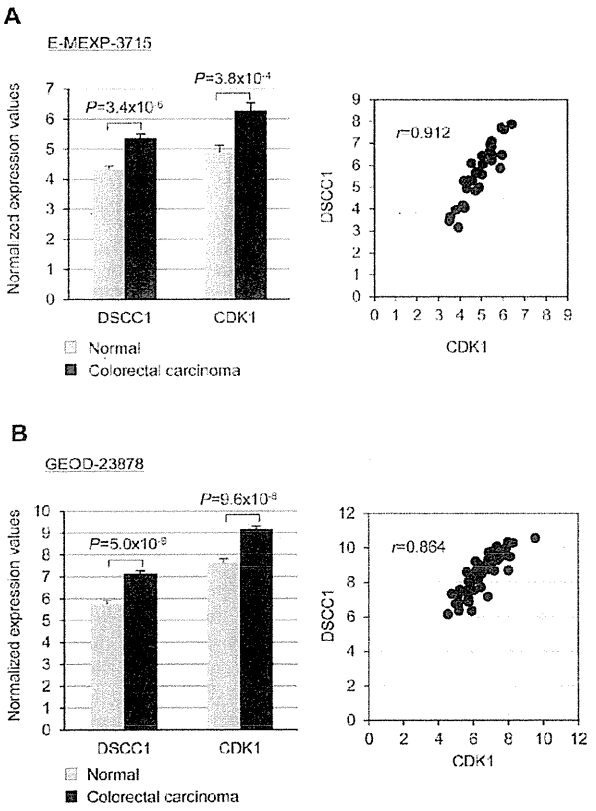

Figure 3. Positive correlation between *DSCC1* and *CDK1* expression in colorectal tumors. This association was shown by two sets of microarray data, E-MEXP-3715 (A) and GEOD-23878 (B), in the Gene Expression Atlas database (http://www.ebi.ac.uk/gxa/). The Pearson's correlation coefficient (r) between *DSCC1* and *CDK1* expression values was then calculated to assess their correlation.
doi:10.1371/journal.pone.0085750.g003

Discussion

Regulated by the retinoblastoma tumor suppressor, pRB, and/or related proteins, E2Fs play crucial roles in cell cycle, nucleotide synthesis, DNA replication, DNA repair, and apoptosis [18,19]. Activities of E2Fs are regulated by integration of signals transduced from the cellular DNA and the external environment. E2F1 is thought to act as an oncogene and a tumor suppressor, with its action dependent on the cellular context. Indeed, overexpression of E2F1 is observed in CRC cells, suggesting its tumorigenic role in the cancer [20]. E2F1 expression is elevated in lung metastasis of colon cancer, and correlates with thymidylate synthase expression, resulting in chemoresistance [21]. On the other hand, E2F1 is over-expressed in colon tumors with increased apoptosis and low proliferation [22]. Therefore, clarification of E2F1 targets should give a clue how this versatile transcription factor family is involved in colorectal carcinogenesis. We have demonstrated here that DSCC1 is frequently up-regulated in CRCs through the transactivation by the E2F family of transcription factors. Although *DSCC1* is located at chromosomal region 8q, which is one of the most frequently amplified chromosomal regions in colorectal tumors [23], copy number gain or amplification was not involved in DSCC1 up-regulation. Instead, we showed here that the flanking region of *DSCC1* transcription start site containing three E2F regulatory sites (EBS1, 2, and 3) plays a role in the transcriptional activation. A previous genome-wide ChIP-chip analysis reported that 20,000 30,000 E2F1-biding sites are distributed over the human genome, of which 51% overlapped transcription start sites [24]. The localization of EBS1, 2, and 3 is compatible with their findings. Among the three sites, EBS1 and EBS3 contain identical sequence with the core E2F1-binding motif (C/GC/GCGC), but EBS2 contains a 1-bp mismatch to the motif. Comparison of human and mouse *DSCC1* 5′-flanking sequences determined that EBS1, located at the −3 to +5 bp region, was well-conserved between the two species (Figure S4A). Consistent with these data, the mutation in EBS1 most remarkably reduced the E2F1-induced promoter activity among the three. Regarding other regulatory elements, we identified a region between −40 and −20 that was associated with basal promoter activity of *DSCC1* (Figure S4B). A search of transcription factor-binding elements in this region found a GC box encompassing a putative ELK1-binding site, but our reporter assay did not show significant change of the promoter activity by ELK1 (data not shown), suggesting that ELK1 may not be involved in the regulation of DSCC1.

Eight members of the mammalian E2F family have been recognized and characterized. Among these members, E2F1, E2F2, and E2F3 are categorized as transcriptional activators, and E2F4, E2F5, E2F6, E2F7, and E2F8 are categorized as repressors [25,26]. In our promoter assay, E2F1, E2F2, E2F3, and E2F4 induced *DSCC1* promoter activity, but E2F6 did not, showing an inconsistent result with E2F4 in the transcription. Molecular studies have uncovered that E2Fs target genes are regulated not only by their binding to DNA element(s) but also by their interacting proteins such as Rb, p107, p130, polycomb group

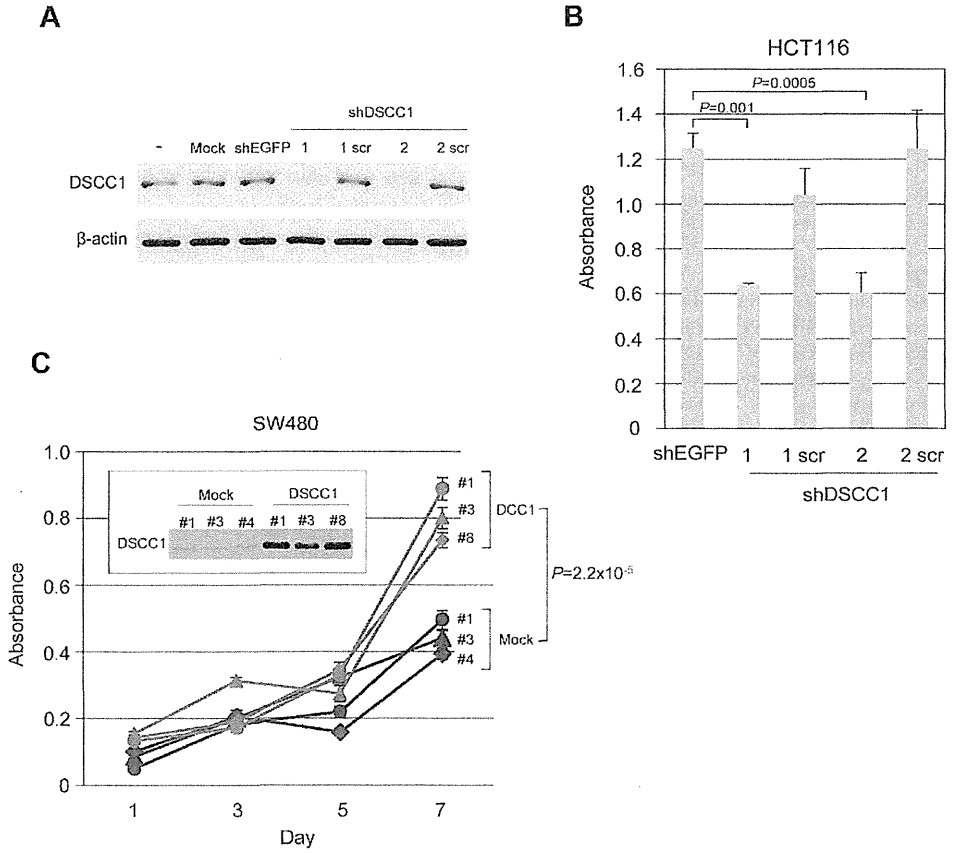

Figure 4. Involvement of DSCC1 in CRC cell proliferation. (A) HCT116 cells were transfected with control (Mock and EGFP) and DSCC1 shRNAs for 48 h using Nucleofector kit, and western blot analysis was performed. Expression of β-actin served as a control. (B) Viability of cells transfected with shRNAs was measured by WST-8 assay. The data represents mean ± SD from three independent transfections. P values were calculated with the Dunnett's test for multiple comparisons to shEGFP-transfected cells. (C) Overexpression of DSCC1 in SW480 cells was confirmed by western blotting using anti-DSCC1 antibody. Equivalent number of three mock and three DSCC1 cells was plated in 96-well plates, and cell proliferation assays were performed at the indicated time points. The data represents mean ± SD from five experiments. A significant difference between mock and DSCC1 cells was determined by two-way repeated measures ANOVA.
doi:10.1371/journal.pone.0085750.g004

proteins, and histone-modification enzymes. Therefore, other factor(s) might affect the elevated promoter activity by E2F4. Although the direct association of E2Fs and their cofactors with the three binding sites needs future detailed analysis, the region containing the three should play a vital role in the elevated expression of DSCC1.

We here showed for the first time that DSCC1 plays an important role in survival of human cancer cells, since enhanced expression of DSCC1 induced survival of cancer cells in response to γ-irradiation, topoisomerase I inhibitor, and DNA-intercalator. The data are consistent with the finding that Dscc1 mutants exhibit sensitivity to γ-irradiation in *Saccharomyces cerevisiae* [27,28]. Another study showed that repair of a topoisomerase I inhibitor-induced DNA double-strand breaks, required components of chromatid cohesion including *Csm3*, *Tof1*, *Mrc1*, and *Dscc1* [29]. Alternatively, DSCC1 may enhance the recombination repair through the CTF18-RFC complex. Our study additionally showed that this resistance seems to be independent of p53 because the induction of apoptosis was also potentiated in HCT116 p53−/− cells (Figure S3F). Associated with CTF8, DSCC1 forms an alternate RFC with CTF18, and further stabilizes 7-subunit complex with RFC2, RFC3, RFC4, and RFC5. Depletion of DSCC1 reduces expression of CTF18, induces decreased replication fork, increases collapse, and suppresses recovery of forks to replication inhibitors, suggesting that DSCC1 is important for DNA replication and recovery from genotoxic insults [30].

Global gene-gene interaction studies have helped gain insights into the complex genetic networks in the yeast. These studies disclosed synthetic lethal combinations of genetic dysfunction, where two genetic variations that have individually no effect on cell viability cause cell death if combined. The concept of synthetic lethality is of great importance in creating therapeutic approaches to selectively kill cancer cells, because genetic and/or epigenetic alterations are expected in cancer cells but not in noncancerous cells. For example, PARP inhibitors have been shown to induce synthetic lethality to cancer cells with BRCA1 or BRCA2 mutations [31,32]. Of note, McLellan and colleagues validated genetic interactions of synthetic lethality in the yeast between *ctf8*, *ctf18*, *dscc1*, *ctf4*, and *rad27* with genes required for the maintenance of chromosomal stability [6]. They additionally showed that these genetic interactions are conserved in *Caenorhabditis elegans*, suggesting the potential utility of these genes for the

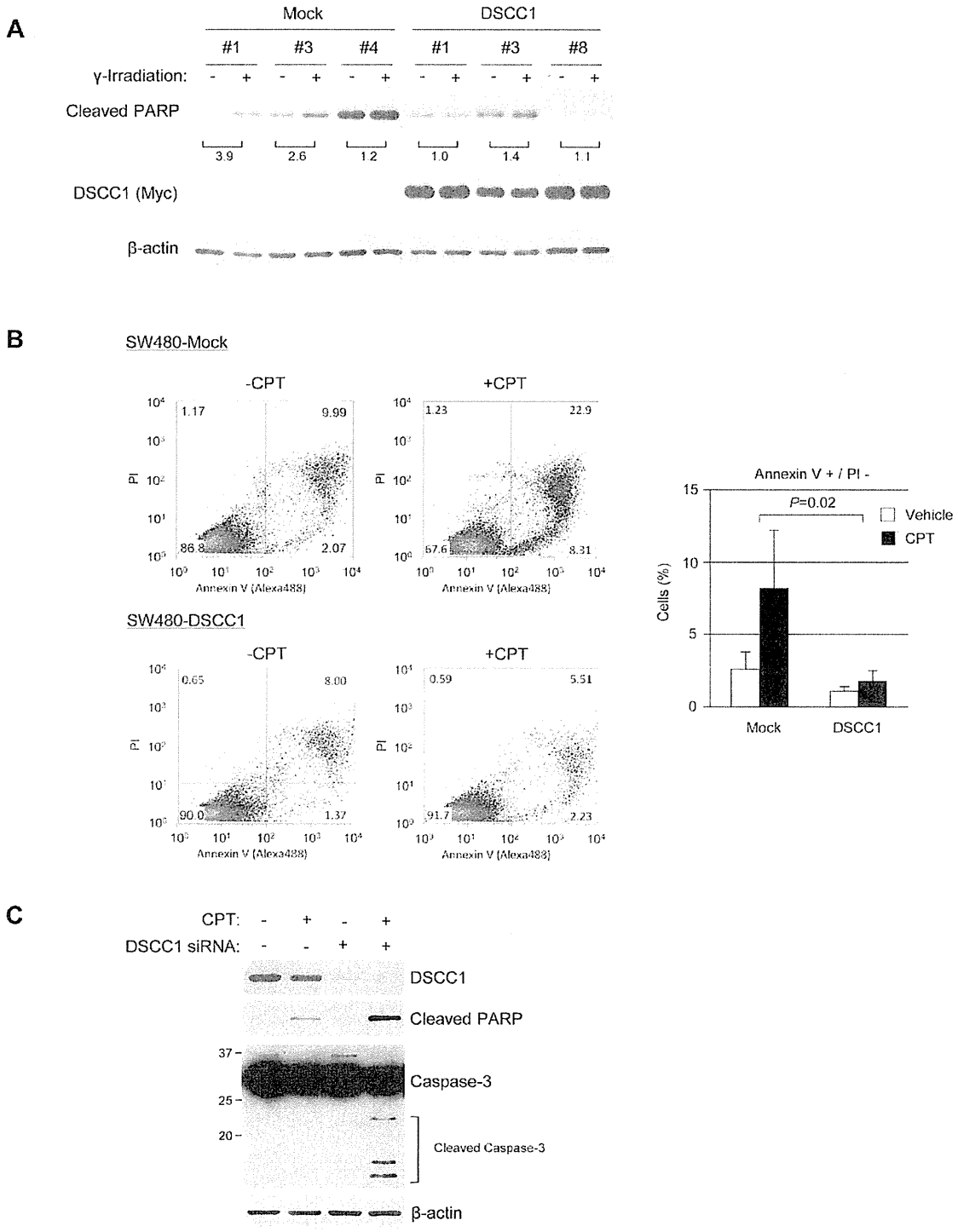

Figure 5. DSCC1 alters sensitivity to apoptotic stimuli. (A) SW480 cells stably expressing DSCC1 or mock (empty vector) were exposed to γ-irradiation (5 Gy). The cells were harvested 24 h after exposure, and the lysates were subjected to western blot analysis. (B) SW480 cells stably expressing DSCC1 or mock were treated with camptothecin (CPT, 30 μM). The cells were harvested 24 h after treatment, and the cell suspensions were subjected to annexin V staining. The data represents mean ± SD from three different clones. Increased annexin V-positive cell population by treatment with CPT was compared between control (Mock) and DSCC1-expressing cells. A significant difference was determined by t-test. (C) HCT116 cells were transfected with control or DSCC1 siRNA, and treated with CPT (30 μM) at 48 h. The cells were harvested 24 h after the CPT-treatment, and the lysates were subjected to western blot analysis.
doi:10.1371/journal.pone.0085750.g005

treatment of colorectal tumors where CIN is frequently involved in the carcinogenesis. They also showed mutations in *ctf4*, *ctf8*, *ctf18*, and *dscc1* are synthetically lethal when combined with mutations in CIN genes including *mre11*, *smc1*, *smc3*, *scc2*, and *pds1* [6]. To test whether CTF18-RFC complex may be associated with chemosensitivity, CTF18, a member of CTF18-RFC complex, was knocked down in HCT116 cells. Interestingly, silencing of CTF18 resulted in the increased cell death in response to camptothecin (Figure S4C). Although further studies on molecular mechanism(s) underlying DSCC1- as well as CTF18-mediated chemoresistance are needed, these data may imply that DSCC1 may facilitate DNA repair through homologous recombination by the regulation of this complex. If this is the case, inhibition of DSCC1 in combination with treatment inducing genotoxic insults such as camptothecin and γ-irradiation may be an effective therapeutic option. Comprehension of DNA damage, repair activities, and anti-apoptotic abilities should be needed to clarify the threshold for apoptosis in each cell.

In summary, our data may give a clue to the understanding of new molecular mechanisms underlying resistance of cancer cells against genotoxic insults, and may contribute to the development of new strategies to overcome the chemoresistance to anti-cancer drugs.

Supporting Information

Figure S1 Subcellular localization of DSCC1. (A) HCT116 and SW480 cells were treated with MG132 (10 μM, 6 h) or cycloheximide (100 μg/ml). The cells were harvested at the indicated time points, and the lysates were subjected to western blot analysis. (B) High magnification images of Figure 1D (x180). (C) HCT116 cells expressing Myc-tagged DSCC1 were probed with anti-Myc antibody followed by FITC-conjugated anti-mouse IgG secondary antibody (green). Nuclei were counter-stained with DAPI (blue). (D) The cytoplasmic and nuclear proteins were analyzed by western blotting.
(TIF)

Figure S2 Regulation of DSCC1 by E2Fs. (A) HEK293T cells were transfected with pcDNA3 HA-E2F1, -E2F2, -E2F3, -E2F4, and -E2F6 for 24 h, and the lysates were subjected to western blot analysis. (B) Chromatin immunoprecipitation was performed using anti-E2F1 antibody. The precipitated DNAs were subjected to the amplification of *CDC2* promoter by quantitative PCR. (C) HeLa cells were transfected with control or E2F1 siRNA (25 nM) for 48 h. Western blot analysis was performed using the indicated antibodies.
(TIF)

Figure S3 DSCC1 alters response to genotoxic insults. (A) Viability of cells transfected with shRNAs was measured by WST-8 assay. The data represents mean ± SD from three to five independent transfections. P values were calculated with the Dunnett's test for multiple comparisons to shEGFP-transfected cells. (B) Overexpression of DSCC1 in HCT116 cells was confirmed by western blot analysis with anti-Flag antibody. Equivalent number of two mock clones, two DSCC1 clones, and parental HCT116 cells was plated in 96-well plates, and these cells were cultured in medium containing 0.5% FBS. Cell proliferation assays were performed at the indicated time points. The data represents mean ± SD from eight experiments. (C) HCT116 cells were treated with control or DSCC1 siRNA (10 nM), followed 48 h later by exposure to γ-irradiation (5 Gy). (D, E) HCT116 cells were treated with control or DSCC1 siRNA (10 nM), followed 48 h later by treatment with doxorubicin (5 μM) or MG132 (2 μM). (F) HCT116 p53-/- cells were treated with control or DSCC1 siRNA (10 nM), followed 48 h later by exposure to γ-irradiation (5 Gy). The cells were harvested 24 h after exposure, and the lysates were subjected to western blot analysis.
(TIF)

Figure S4 Alignment of human and mouse *DSCC1* 5′-flanking sequence. (A) Alignment of human and mouse *DSCC1* 5′-flanking sequence by the DBTSS database (http://dbtss.hgc.jp/). Top strand represents the 5′-flanking sequences of human *DSCC1*, and the bottom strand represents the 5′-flanking sequences of mouse *Dscc1*. E2F binding motifs are underlined. (B) pDSCC1-133/+109 or the shorter promoter constructs was transfected with pRL-TK into SW480 cells. The promoter activity was measured by luciferase activity. Each value represents mean ± SD from three independent transfections. (C) The effect of CTF18 siRNA (S: 5′-CCAACUGCCUGGUCAUCG-3′, AS: 5′-UCGAUGACCAGGCAGUUG-3′) was evaluated by quantitative PCR (CTF18 primers, forward: 5′-CTTCTCGGTGTGGCAGGA-3′, reverse: 5′-CAGCAGGAGTGTGTCAGCAG-3′). HCT116 cells were treated with control or CTF18 siRNA (10 nM), followed 48 h later by treatment with CPT (30 μM). The cells were harvested 24 h after treatment, and the lysates were subjected to western blot analysis.
(TIF)

Table S1 Correlations between DSCC1 expression and the clinicopathological characteristics of the 40 colon cancer patients.
(XLS)

Acknowledgments

We thank Masashi Miura, Seira Hatakeyama, and Hiromi Toyoda (The University of Tokyo) for their technical assistance and Yumiko Ishii (IMSUT FACS Core Laboratory) for the assistance of flow cytometry.

Author Contributions

Conceived and designed the experiments: KY YF. Performed the experiments: KY NT. Analyzed the data: RY AN SI SM. Contributed reagents/materials/analysis tools: TI TF MS GT KH YN. Wrote the paper: KY YF.

References

1. Rajagopalan H, Nowak MA, Vogelstein B, Lengauer C (2003) The significance of unstable chromosomes in colorectal cancer. Nat Rev Cancer 3: 695–701.
2. Wang Z, Cummins JM, Shen D, Cahill DP, Jallepalli PV, et al. (2004) Three classes of genes mutated in colorectal cancers with chromosomal instability. Cancer Res 64: 2998–3001.
3. Barber TD, McManus K, Yuen KW, Reis M, Parmigiani G, et al. (2008) Chromatid cohesion defects may underlie chromosome instability in human colorectal cancers. Proc Natl Acad Sci U S A 105: 3443–3448.
4. Mayer ML, Gygi SP, Aebersold R, Hieter P (2001) Identification of RFC(Ctf18p, Ctf8p, Dcc1p): an alternative RFC complex required for sister chromatid cohesion in S. cerevisiae. Mol Cell 7: 959–970.
5. Lin YM, Furukawa Y, Tsunoda T, Yue CT, Yang KC, et al. (2002) Molecular diagnosis of colorectal tumors by expression profiles of 50 genes expressed differentially in adenomas and carcinomas. Oncogene 21: 4120–4128.
6. McLellan J, O'Neil N, Tarailo S, Stoepel J, Bryan J, et al. (2009) Synthetic lethal genetic interactions that decrease somatic cell proliferation in Caenorhabditis elegans identify the alternative RFC CTF18 as a candidate cancer drug target. Mol Biol Cell 20: 5306–5313.
7. Bermudez VP, Maniwa Y, Tappin I, Ozato K, Yokomori K, et al. (2003) The alternative Ctf18-Dcc1-Ctf8-replication factor C complex required for sister chromatid cohesion loads proliferating cell nuclear antigen onto DNA. Proc Natl Acad Sci U S A 100: 10237–10242.

8. Pan X, Ye P, Yuan DS, Wang X, Bader JS, et al. (2006) A DNA integrity network in the yeast Saccharomyces cerevisiae. Cell 124: 1069 1081.
9. Tong AH, Lesage G, Bader GD, Ding H, Xu H, et al. (2004) Global mapping of the yeast genetic interaction network. Science 303: 808 813.
10. Gellon L, Razidlo DF, Gleeson O, Verra L, Schulz D, et al. (2011) New functions of Ctf18-RFC in preserving genome stability outside its role in sister chromatid cohesion. PLoS Genet 7: e1001298.
11. Yamaguchi K, Sakai M, Shimokawa T, Yamada Y, Nakamura Y, et al. (2010) C20orf20 (MRG-binding protein) as a potential therapeutic target for colorectal cancer. Br J Cancer 102: 325 331.
12. Shimokawa T, Furukawa Y, Sakai M, Li M, Miwa N, et al. (2003) Involvement of the FGF18 gene in colorectal carcinogenesis, as a novel downstream target of the beta-catenin/T-cell factor complex. Cancer Res 63: 6116 6120.
13. Zheng N, Fraenkel E, Pabo CO, Pavletich NP (1999) Structural basis of DNA recognition by the heterodimeric cell cycle transcription factor E2F-DP. Genes Dev 13: 666 674.
14. Xu X, Bieda M, Jin VX, Rabinovich A, Oberley MJ, et al. (2007) A comprehensive ChIP-chip analysis of E2F1, E2F4, and E2F6 in normal and tumor cells reveals interchangeable roles of E2F family members. Genome Res 17: 1550 1561.
15. Hirano G, Izumi H, Kidani A, Yasuniwa Y, Han B, et al. (2010) Enhanced expression of PCAF endows apoptosis resistance in cisplatin-resistant cells. Mol Cancer Res 8: 864 872.
16. Wikonkal NM, Remenyik E, Knezevic D, Zhang W, Liu M, et al. (2003) Inactivating E2f1 reverts apoptosis resistance and cancer sensitivity in Trp53-deficient mice. Nat Cell Biol 5: 655 660.
17. Zheng C, Ren Z, Wang H, Zhang W, Kalvakolanu DV, et al. (2009) E2F1 Induces tumor cell survival via nuclear factor-kappaB-dependent induction of EGR1 transcription in prostate cancer cells. Cancer Res 69: 2324 2331.
18. Nevins JR (2001) The Rb/E2F pathway and cancer. Hum Mol Genet 10: 699 703.
19. Wong JV, Dong P, Nevins JR, Mathey-Prevot B, You L (2011) Network calisthenics: control of E2F dynamics in cell cycle entry. Cell Cycle 10: 3086 3094.
20. Suzuki T, Yasui W, Yokozaki H, Naka K, Ishikawa T, et al. (1999) Expression of the E2F family in human gastrointestinal carcinomas. International journal of cancer Journal international du cancer 81: 535 538.
21. Banerjee D, Gorlick R, Liefshitz A, Danenberg K, Danenberg PC, et al. (2000) Levels of E2F-1 expression are higher in lung metastasis of colon cancer as compared with hepatic metastasis and correlate with levels of thymidylate synthase. Cancer Res 60: 2365 2367.
22. Zacharatos P, Kotsinas A, Evangelou K, Karakaidos P, Vassiliou LV, et al. (2004) Distinct expression patterns of the transcription factor E2F-1 in relation to tumour growth parameters in common human carcinomas. J Pathol 203: 744 753.
23. Meijer GA, Hermsen MA, Baak JP, van Diest PJ, Meuwissen SG, et al. (1998) Progression from colorectal adenoma to carcinoma is associated with non-random chromosomal gains as detected by comparative genomic hybridisation. J Clin Pathol 51: 901 909.
24. Bieda M, Xu X, Singer MA, Green R, Farnham PJ (2006) Unbiased location analysis of E2F1-binding sites suggests a widespread role for E2F1 in the human genome. Genome Res 16: 595 605.
25. DeGregori J, Johnson DG (2006) Distinct and Overlapping Roles for E2F Family Members in Transcription, Proliferation and Apoptosis. Curr Mol Med 6: 739 748.
26. Iaquinta PJ, Lees JA (2007) Life and death decisions by the E2F transcription factors. Curr Opin Cell Biol 19: 649 657.
27. Bennett CB, Lewis LK, Karthikeyan G, Lobachev KS, Jin YH, et al. (2001) Genes required for ionizing radiation resistance in yeast. Nat Genet 29: 426 434.
28. Game JC, Williamson MS, Baccari C (2005) X-ray survival characteristics and genetic analysis for nine Saccharomyces deletion mutants that show altered radiation sensitivity. Genetics 169: 51 63.
29. Redon C, Pilch DR, Bonner WM (2006) Genetic analysis of Saccharomyces cerevisiae H2A serine 129 mutant suggests a functional relationship between H2A and the sister-chromatid cohesion partners Csm3-Tof1 for the repair of topoisomerase I-induced DNA damage. Genetics 172: 67 76.
30. Terret ME, Sherwood R, Rahman S, Qin J, Jallepalli PV (2009) Cohesin acetylation speeds the replication fork. Nature 462: 231 234.
31. Bryant HE, Schultz N, Thomas HD, Parker KM, Flower D, et al. (2005) Specific killing of BRCA2-deficient tumours with inhibitors of poly(ADP-ribose) polymerase. Nature 434: 913 917.
32. Farmer H, McCabe N, Lord CJ, Tutt AN, Johnson DA, et al. (2005) Targeting the DNA repair defect in BRCA mutant cells as a therapeutic strategy. Nature 434: 917 921.

安井　寛
(東京大学)

Biol Blood Marrow Transplant xxx (2014) 1–5

High Level of Serum Soluble Interleukin-2 Receptor at Transplantation Predicts Poor Outcome of Allogeneic Stem Cell Transplantation for Adult T Cell Leukemia

Akio Shigematsu [1,*], Naoki Kobayashi [2], Hiroshi Yasui [3], Motohiro Shindo [4], Yasutaka Kakinoki [5], Kyuhei Koda [6], Satoshi Iyama [7], Hiroyuki Kuroda [8], Yutaka Tsutsumi [9], Masahiro Imamura [2], Takanori Teshima [1]

[1] *Department of Hematology, Hokkaido University, Sapporo, Japan*
[2] *Department of Hematology, Sapporo Hokuyu Hospital, Sapporo, Japan*
[3] *First Department of Internal Medicine, Sapporo Medical University, Sapporo, Japan*
[4] *Third Department of Internal Medicine, Asahikawa Medical School, Asahikawa, Japan*
[5] *Department of Hematology, Asahikawa City Hospital, Asahikawa, Japan*
[6] *Department of Hematology and Oncology, Asahikawa Red Cross Hospital, Asahikawa, Japan*
[7] *Fourth Department of Internal Medicine, Sapporo Medical University, Sapporo, Japan*
[8] *Department of Hematology and Oncology, Steel Memorial Muroran Hospital, Muroran, Japan*
[9] *Department of Internal Medicine, Hakodate Municipal Hospital, Hakodate, Japan*

Article history:
Received 8 January 2014
Accepted 17 February 2014

Key Words:
Adult T cell leukemia
Allogeneic stem cell transplantation
Region-wide study
Soluble interleukin-2 receptor
Prognostic factor

A B S T R A C T

The prognosis for adult T cell leukemia/lymphoma (ATL) is very poor, and only allogeneic hematopoietic stem cell transplantation (allo-SCT) has been considered to be a curative treatment for ATL. In this study, we retrospectively analyzed data for patients who had received allo-SCT for ATL in Hokkaido, the northernmost island of Japan, to determine prognostic factors. Fifty-six patients with a median age of 57 years received allo-SCT. Twenty-eight (50.0%) patients had acute type and 22 (46.4%) had lymphoma type. Twenty-three (41.1%) patients received allo-SCT in complete remission (CR), whereas the others were in non-CR. Seventeen (30.4%) patients received myeloablative conditioning and the others received reduced-intensity conditioning. With a median follow-up period of 48 months (range, 17 to 134 months), 1-year overall survival (OS) and 5-year OS rates were 55.4% and 46.1%, respectively. The survival curve reached a plateau at 22 months after stem cell transplantation (SCT). Male sex, high level of serum soluble interleukin-2 receptor (sIL-2R) at SCT, and non-CR at SCT were determined to be significant risk factors for OS. A high level of sIL-2R at SCT was a risk factor for poor OS in patients with non-CR at SCT by univariate analysis ($P = .02$), and it remained significant after adjustment by sex (hazard ratio, 2.73 [95% confidence interval, 1.07 to 7.90]). A high level of sIL-2R at SCT was also determined to be a risk factor for disease progression ($P = .02$). This region-wide study showed encouraging results for survival after allo-SCT for ATL and demonstrated for the first time that a high level of sIL-2R at SCT predicts worse SCT outcome.

INTRODUCTION

Adult T cell leukemia/lymphoma (ATL) is a peripheral T cell lymphoma caused by human T cell lymphotropic virus type 1 (HTLV-1), and the prognoses of aggressive subtypes (acute type and lymphoma type) of ATL are very poor [1]. Although only allogeneic hematopoietic stem cell transplantation (allo-SCT) has been considered to be a curative treatment for aggressive subtypes of ATL [2], less than 40% of patients who have received allo-SCT have been cured [3-5]. We previously reported excellent outcomes for ATL patients who received allo-SCT from 2 institutions in Hokkaido, the northernmost island of Japan [6], and overall survival (OS) rate in that study was 73.3% at 3 years after allo-SCT. We, therefore, conducted a region-wide retrospective study in this area to determine prognostic factors for patients with ATL who received allo-SCT.

PATIENTS AND METHODS

Collection of Data

Clinical data for 56 patients who received allo-SCT for ATL between January 2000 and March 2012 were collected from all stem cell transplantation (SCT) centers in Hokkaido, Japan. The patients included all patients with ATL who received allo-SCT in this area. This study was conducted with the approval of the institutional review board of Hokkaido University Hospital. Conditioning regimens and other procedures of SCT were performed according to the decision of the clinicians at each center.

Definitions

Shimoyama's classification was used for the definition of ATL subtypes [7]. Neutrophil engraftment and platelet engraftment were defined as the first of 3 days with absolute neutrophil count > .5 × 10^9/L and the first of 7 days with an untransfused platelet count > 50 × 10^9/L, respectively. The hematopoietic cell transplant comorbidity index was scored by the criteria previously described [8]. Acute graft-versus-host disease (AGVHD) and chronic GVHD (CGVHD) were graded by standard criteria [9,10]. Transplantation-related mortality (TRM) was defined as any death other than death from ATL. OS was calculated from the day of SCT until death or last follow-up. Progression of ATL was defined as relapse after remission, development of new lesions, or increase in measurable disease or in the number of

Financial disclosure: See Acknowledgments on page 5.

* Correspondence and reprint requests: Akio Shigematsu, MD, PhD, Department of Hematology, Hokkaido University Graduate School of Medicine, Kita-15 Nishi-7, Kita-ku, Sapporo, Hokkaido, 060-8638, Japan.
E-mail address: shigema@med.hokudai.ac.jp (A. Shigematsu).

1083-8791/$ – see front matter © 2014 American Society for Blood and Marrow Transplantation.
http://dx.doi.org/10.1016/j.bbmt.2014.02.014

circulating leukemic cells by 25% or more [11]. Progression-free survival (PFS) was defined as survival without progression of ATL.

Endpoint and Statistical Analysis

The primary endpoint of this study was OS rate of the patients. Descriptive statistical analysis was performed using the chi-square test or Fisher's exact test as appropriate for categorical variables and using the 2-sided Wilcoxon rank-sum test for continuous variables. The probabilities of OS and PFS were estimated using the Kaplan-Meier method. Disease progression rates and TRM rates were estimated using cumulative incidence analysis and considered as competing risks, and Gray's test was used for group comparison of cumulative incidence. The effects of various patient and disease categorical variables on survival probabilities were examined using the log-rank test, and the following variables were included in subgroup analyses: age of the patients, sex of the patients, levels of serum soluble interleukin-2 receptor (sIL-2R) at diagnosis and SCT, disease status at SCT, disease subtypes, months from diagnosis to SCT, levels of lactate dehydrogenase (LDH) at diagnosis and at SCT, donor, stem cell source, intensity of the conditioning regimen, GVHD prophylaxis, and CGVHD. All P values were 2-sided and a P value of .05 was used as the cutoff for statistical significance. Multivariate analysis for OS was performed using the Cox proportional hazards regression model.

RESULTS

Patients and Transplantation Characteristics

Patients and SCT characteristics are summarized in Table 1. The median age of the patients was 57 years, and one half of the patients were male. Twenty-eight (50.0%) patients had acute type and 22 (46.4%) patients had lymphoma type. HTLV-1 serostatus of donors were available in 47 patients, and only 2 (4.3%) donors were positive for HTLV-1. After induction chemotherapies that were mainly CHOP or VCAP-AMP-VECP regimens [12], 23 (41.1%) patients received allo-SCT in complete remission (CR) and 33 (58.9%) patients received allo-SCT in non-CR. Nineteen patients had high level of sIL-2R at SCT. Among the patients with high level of sIL-2R at SCT, only 1 patient was in CR at SCT and the other 18 patients were not in CR at SCT. There was a correlation between disease status at SCT and sIL-2R at SCT (median, 824 U/mL [range, 351 to 2530] in CR patients versus a median of 2325 U/mL [range, 435 to 37,384 U/mL] in non-CR patients; P = .02). Seventeen (30.4%) patients received myeloablative conditioning, which consisted of high-dose cyclophosphamide and total body irradiation with or without VP-16, and 39 (69.6%) patients received reduced-intensity conditioning, which consisted of fludarabine with either busulfan or melphalan ±low-dose total body irradiation of 2 to 4 Gray.

Table 1
Patient and Transplantation Characteristics

Characteristics (n = 56)	Value
Age, median (range), yr	57 (37-69)
Age ≥ 60	37 (66.1%)
Sex	
Male	28 (50.0%)
Female	28 (50.0%)
Disease subtype	
Acute	28 (50.0%)
Lymphoma	26 (46.4%)
Chronic	1 (1.8%)
Smoldering	1 (1.8%)
WBC count at diagnosis, median (range), per μL	10,900 (2500-331,000)
LDH level at diagnosis, median (range), IU/L	352 (144-1736)
sIL-2R level at diagnosis, median (range), per mL	11,153 (998-116,100)
Months from diagnosis to SCT, median (range)	196 (60-3690)
≤ 3 months	7 (12.5%)
3-6 months	17 (30.4%)
> 6 months	32 (57.1%)
Disease status at SCT	
CR	23 (41.1%)
Non-CR	33 (58.9%)
PR	19 (33.9%)
REF	10 (17.9%)
REL	4 (7.1%)
LDH level at diagnosis, median (range), IU/L	218 (150-766)
sIL-2R level at SCT, median (range), U/mL	1219 (351-37,387)
HCT-CI score*	
0	22 (41.5%)
1	11 (20.8%)
2	9 (17.0%)
3	6 (11.3%)
4-7	5 (9.4%)
Donor	
MRD	20 (35.7%)
MUD	22 (39.3%)
MMD	14 (25.0%)
Sex disparity	
Match	32 (57.1%)
Mismatch	24 (42.9%)
Male to female	15 (26.8%)
Female to male	9 (16.1%)
Stem cell source	
BM	39 (69.6%)
PBSC†	11 (19.6%)
CB	6 (10.7%)
Conditioning regimen	
MAC	17 (30.4%)
RIC	39 (69.6%)
TBI	
Yes	40 (71.4%)
No	16 (28.6%)
GVHD prophylaxis	
CSP+MTX	22 (39.3%)
TK+MTX	25 (44.6%)
CSP alone or TK alone	7 (12.5%)

WBC indicates white blood cell; LDH, lactate dehydrogenase; SCT, stem cell transplantation; sIL-2R, soluble interleukin-2 receptor; CR, complete remission; PR, partial remission; REF, primary refractory; REL, relapse; MRD, HLA-matched related donor; MUD, HLA-matched unrelated donor; MMD, HLA-mismatched donor; BM, bone marrow; PBSC, peripheral blood stem cell; CB, cord blood; MAC, myeloablative conditioning; RIC, reduced-intensity conditioning; LDH lactate dehydrogenase; HCT-CI, hematopoietic cell transplant comorbidity index; TBI, Total body irradiation; GVHD, graft-versus-host disease; CSP, cyclosporin A; MTX, methotrexate; TK, tacrolimus. Data presented are n (%) unless otherwise indicated.

* HCT-CI score was not available in 3 patients.

† PBSC were from an MRD in all cases because donation of PBSC from unrelated donors is not permitted in Japan until 2010.

Transplantation Outcomes

Engraftment and GVHD

Except for 3 patients who died before engraftment, 53 (94.6%) patients achieved neutrophil engraftment at a median of 16 (range, 9 to 31) days. Platelet engraftment could be assessed in 52 patients, and 40 (76.9%) patients achieved platelet engraftment at a median of 27 (range, 14 to 415) days. All patients who achieved neutrophil engraftment were assessed for AGVHD. Overall AGVHD, grade II to IV AGVHD, and grade III to IV AGVHD occurred in 40 (75.5%), 31 (58.5%), and 8 (15.1%) of the evaluable patients, respectively. The median onset of AGVHD was 29 (range, 8 to 101) days. CGVHD was assessed in 43 patients who survived beyond day 100 after SCT. CGVHD occurred in 24 (55.8%) of the evaluable patients at a median onset day of 168 (range, 69 to 495) days, and extensive CGVHD occurred in 16 patients (37.2%).

Disease progression and TRM

Cumulative incidences of disease progression and TRM are shown in Figure 1. Fourteen (25.0%) patients showed disease progression at a median of 74 (range, 12 to 273) days after SCT. Twelve patients with disease progression after SCT died of ATL. One of the other 2 patients with disease progression died of a transplantation-related complication in

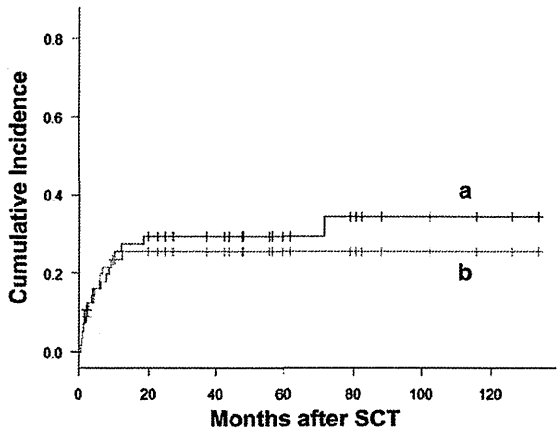

Figure 1. Cumulative incidence analyses of disease progression and TRM after SCT. Cumulative incidences of (a) TRM and (b) disease progression after allo-SCT. Disease progression and TRM were considered as competing risks.

remission and the other is alive in remission. The median time from disease progression to death was 92 (range, 32 to 399) days. Eighteen (32.1%) patients died of TRM at a median of 148 (range, 12 to 2143) days. The causes of TRM included infection (n = 6), AGVHD (n = 4), veno-occlusive disease (n = 2), CGVHD (n = 2), thrombotic microangiopathy (n = 1), cerebral infarction (n = 1), chronic renal failure (n = 1), and suicide (n = 1). Univariate analysis showed that a high level of sIL-2R at SCT (≥ 2000 U/mL) was significantly associated with disease progression ($P = .02$), whereas male sex tended to be associated with increased risk ($P = .06$). Non-CR at SCT was marginally significant for TRM ($P = .07$).

Survival

The median follow-up period for survivors was 48 (range, 17 to 134) months. One-year OS and 5-year OS rates were 55.4% and 46.1%, respectively. One-year PFS and 5-year PFS were 51.1% and 45.6%, respectively. The survival curve reached a plateau at 22 months after SCT (Figure 2). Male sex ($P = .002$), a high level of sIL-2R both at diagnosis (≥ 10,000 U/mL, $P =$

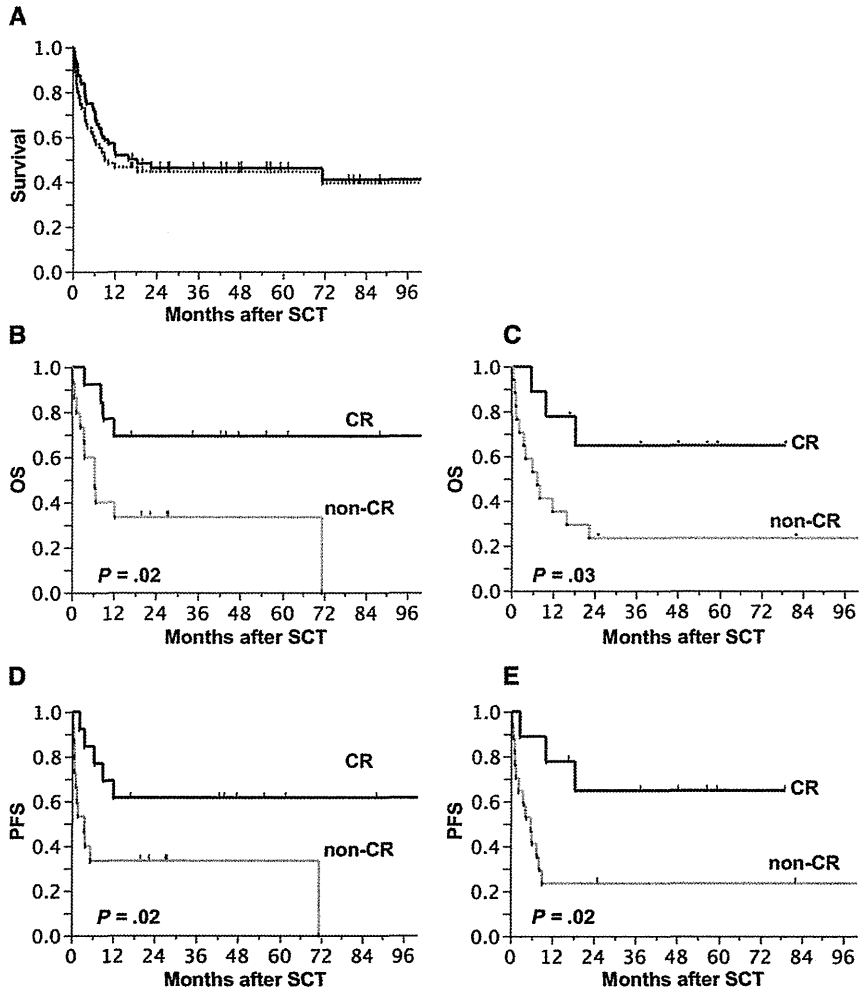

Figure 2. Survival after SCT. (A) Overall survival and progression-free survival after SCT in all patients. The solid line shows the overall survival curve and the dotted line shows the progression-free survival curve. (B) Overall survival in patients with acute type according to disease status at SCT. (C) Overall survival in patients with lymphoma type according to disease status at SCT. (D) Progression-free survival in patients with acute type according to disease status at SCT. (E) Progression-free survival in patients with lymphoma type according to disease status at SCT.

.02) and at SCT (≥ 2000 U/mL, $P < .001$) (Figure 3), and non-CR at SCT ($P < .001$) were identified as significant risk factors for OS by univariate analyses. Disease subtypes and other factors were not risk factors for OS. We tested several cutoff points of sIL-2R for determining the most significant cutoff points for survival and found that the cutoff levels of 10,000 at diagnosis and 2000 at SCT were most significantly associated with survival. Worse survival for male patients and patients in non-CR at SCT were confirmed by using multivariate analysis (hazard ratio, 3.40 [95% confidence interval (CI), 1.44 to 8.02] for male patients; hazard ratio, 4.45 [95% CI, 1.82 to 10.87] for non-CR patients). The levels of sIL-2R at SCT were not included in multivariate analysis, which included disease status, because the levels of sIL-2R at SCT were correlated with the disease status at SCT. In patients in non-CR at SCT, the level of sIL-2R was significantly associated with OS ($P = .02$) (Figure 3B), regardless of disease subtype ($P = .02$ for acute type and $P = .01$ for lymphoma type) (Figure 3C,D), and a high level of sIL-2R at SCT was determined to be a prognostic factor when it was used as an alternative variable to disease status at SCT in multivariate analysis (hazard ratio, 5.95 [95% CI, 2.14 to 17.9]). We performed multivariate analysis for non-CR patients using a level of sIL-2R at SCT and sex of the patients as variables, and a high level of sIL-2R at SCT remained significant even after adjustment by sex of the patients (hazard ratio, 2.73 [95% CI, 1.07 to 7.90]). The other variables were not confirmed to be significant by multivariate analysis.

DISCUSSION

A previous retrospective study on allo-SCT for ATL in Japan [4] demonstrated 3-year OS of 36.0%, and a prospective study on allo-SCT using a reduced-intensity conditioning regimen showed 5-year OS of 34.0% [5]. The 5-year OS rate in the present study was 46.1% and the survival curve reached a plateau at 22 months after SCT. Although the results of the present study are worse than the results we previously reported [6], the difference in results is probably due to the selection bias of the patients or might simply reflect a multi-institutional study versus a selected institutional study.

In previous nationwide studies on ATL in Japan, advanced age, male sex, non-CR at SCT, poor performance status, SCT from unrelated donors, or SCT using cord blood were associated with poor survival after allo-SCT [3,4]. Multivariate analysis in this study confirmed that male patients and patients in non-CR at SCT were at risk for poor OS. There were no differences in characteristics of the patients and SCT between male and female patients (data not shown), and the incidence of disease progression after allo-SCT was increased in male patients with marginal significance ($P = .06$). There has been no report showing worse survival in male patients after chemotherapy for ATL. It is thus tempting to speculate that this difference is due to the difference in allogeneic immune responses between male and female recipients after allo-SCT.

Although a high level of sIL-2R has been reported to reflect disease progression of ATL [13,14], the clinical significance of sIL-2R for patients who received allo-SCT remains to be determined. In this study, a high level of sIL-2R at SCT was identified as a significant risk factor for OS by univariate analysis. We did not include sIL-2R at SCT in the multivariate analysis because the level of sIL-2R at SCT was stringently correlated with disease status at SCT. However, a high level of sIL-2R at SCT was determined to be a prognostic factor when it was used as an alternative variable to disease status at SCT in multivariate analysis, and a high level of sIL-2R at SCT was a risk factor for OS in patients with non-CR at SCT, regardless of the sex of the patient. Only sIL-2R at SCT was identified as a risk factor for disease progression. Thus, sIL-2R at SCT could be a useful surrogate marker for disease status. Although transplantation outcomes in non-CR patients were inferior to those in CR patients, as has been previously reported [3,4], the level of sIL-2R at SCT was significantly associated with OS in non-CR patients, indicating that sIL-2R level at SCT could be used as a decision-making parameter for selection of allo-SCT for patients in non-CR. Additional chemotherapies or a

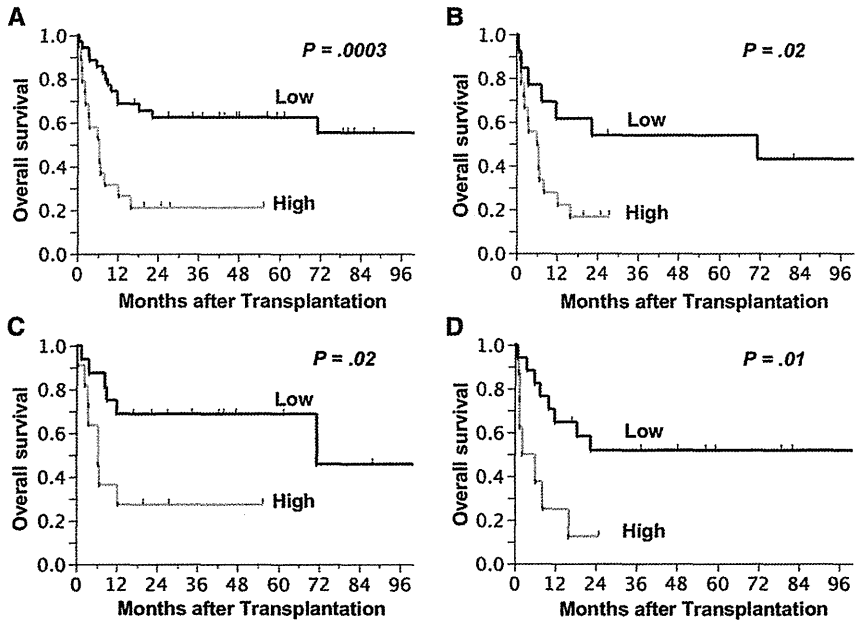

Figure 3. Overall survival according to level of serum sIL-2R at SCT. A high level of serum sIL-2R at SCT was defined as 2000 U/mL or higher. (A) All patients. (B) Patients who were in non-CR at SCT. (C) Patients with acute type of ATL. (D) Patients with lymphoma type of ATL.

novel anti-CCR4 antibody therapy [15] before SCT for patients who have high level of sIL-2R may improve the outcome of allo-SCT, although this hypothesis needs to be tested in a prospective study.

In conclusion, although the current study has several limitations that should be considered when reviewing the findings, including the use of a retrospective design and a small number of patients, it showed encouraging results of allo-SCT for patients with ATL in both CR and non-CR with low levels of sIL-2R at SCT.

ACKNOWLEDGMENTS

Financial disclosure: The authors have nothing to disclose.

Conflict of interest statement: There are no conflicts of interest to report.

REFERENCES

1. Vose J, Armitage J, Weisenburger D. International T-Cell Lymphoma Project. International peripheral T-cell and natural killer/T-cell lymphoma study: pathology findings and clinical outcomes. *J Clin Oncol.* 2008;26:4124-4130.
2. Bazarbachi A, Suarez F, Fields P, Hermine O. How I treat adult T-cell leukemia/lymphoma. *Blood.* 2011;18:1736-1745.
3. Hishizawa M, Kanda J, Utsunomiya A, et al. Transplantation of allogeneic hematopoietic stem cells for adult T-cell leukemia: a nationwide retrospective study. *Blood.* 2010;116:1369-1376.
4. Ishida T, Hishizawa M, Kato K, et al. Allogeneic hematopoietic stem cell transplantation for adult T-cell leukemia-lymphoma with special emphasis on preconditioning regimen: a nationwide retrospective study. *Blood.* 2012;120:1734-1741.
5. Choi I, Tanosaki R, Uike N, et al. ATLL allo-HSCT Study Group. Long-term outcomes after hematopoietic SCT for adult T-cell leukemia/lymphoma: results of prospective trials. *Bone Marrow Transplant.* 2011; 46:116-118.
6. Shiratori S, Yasumoto A, Tanaka J, et al. A retrospective analysis of allogeneic hematopoietic stem cell transplantation for adult T cell leukemia/lymphoma (ATL): clinical impact of graft-versus-leukemia/lymphoma effect. *Biol Blood Marrow Transplant.* 2008;14:817-823.
7. Shimoyama M. Diagnostic criteria and classification of clinical subtypes of adult T-cell leukaemia lymphoma. A report from the Lymphoma Study Group (1984-87). *Br J Haematol.* 1991;79:428-437.
8. Sorror ML, Maris MB, Storb R, et al. Hematopoietic cell transplantation (HCT)-specific comorbidity index: a new tool for risk assessment before allogeneic HCT. *Blood.* 2005;106:2912-2919.
9. Przepiorka D, Weisdorf D, Martin P, et al. 1994 Consensus Conference on Acute GVHD Grading. *Bone Marrow Transplant.* 1995;15: 825-828.
10. Sullivan KM, Agura E, Anasetti C, et al. Chronic graft-versus host disease and other late complications of bone marrow transplantation. *Semin Hematol.* 1991;28:250-259.
11. Gill PS, Harrington W Jr, Kaplan MH, et al. Treatment of adult T-cell leukemia-lymphoma with a combination of interferon alfa and zidovudine. *N Engl J Med.* 1995;332:1744-1748.
12. Tsukasaki K, Utsunomiya A, Fukuda H, et al. VCAP-AMP-VECP compared with biweekly CHOP for adult T-cell leukemia-lymphoma: Japan Clinical Oncology Group Study JCOG9801. *J Clin Oncol.* 2007;25: 5458-5464.
13. Kamihira S, Atogami S, Sohda H, et al. Significance of soluble interleukin-2 receptor levels for evaluation of the progression of adult T-cell leukemia. *Cancer.* 1994;73:2753-2758.
14. Yasuda N, Lai PK, Ip SH, et al. Soluble interleukin 2 receptors in sera of Japanese patients with adult T cell leukemia mark activity of disease. *Blood.* 1988;71:1021-1026.
15. Ishida T, Joh T, Uike N, et al. Defucosylated anti-CCR4 monoclonal antibody (KW-0761) for relapsed adult T-cell leukemia-lymphoma: a multicenter phase II study. *J Clin Oncol.* 2012;30:837-842.

Epstein-Barr Virus–infected Cells in IgG4-related Lymphadenopathy With Comparison With Extranodal IgG4-related Disease

Mai Takeuchi, MB,† Yasuharu Sato, MD,* Hiroshi Yasui, MD,‡ Hiroaki Ozawa, MD,§ Kyotaro Ohno, MB,* Katsuyoshi Takata, MD,* Yuka Gion, MHS,* Yorihisa Orita, MD,‖ Tomoyasu Tachibana, MB,¶ Tomoo Itoh, MD,† Naoko Asano, MD,# Shigeo Nakamura, MD,** Steven H. Swerdlow, MD,†† and Tadashi Yoshino, MD**

Abstract: IgG4-related lymphadenopathy with increased numbers of Epstein-Barr virus (EBV)-infected cells has been reported but not fully described. We analyzed 31 cases of IgG4-related lymphadenopathy and 24 cases of extranodal IgG4-related diseases for their possible relationship with EBV. Other types of reactive lymph nodes (22) and angioimmunoblastic T-cell lymphoma (AITL) (10) were also studied for comparison. EBV-encoded RNA (EBER) in situ hybridization revealed EBER$^+$ cells in 18 of 31 cases (58%) of IgG4-related lymphadenopathy. Increased EBER$^+$ cells were found in only 4 of 22 (18.1%) non–IgG4-related reactive lymphoid hyperplasia in patients of a similar age ($P = 0.002$) and in only 5 of 24 (21%) extranodal IgG4-related biopsies ($P = 0.006$). Interestingly, all patients with EBER$^+$ progressively transformed germinal center–type IgG4-related lymphadenopathy had systemic lymphadenopathy and/or extranodal involvement. AITL also is associated with EBV, and IgG4-related lymphadenopathy sometimes mimics the morphology of AITL; however, the number of IgG4$^+$ cells in AITL was significantly less than that in IgG4-related lymphadenopathy ($P < 0.001$). Increased numbers of regulatory T cells are seen in IgG4-related disease; however, there was not a significant difference between the EBER$^+$ and EBER$^-$ cases. In conclusion, the presence of increased numbers of EBV-infected cells in IgG4-related lymphadenopathy, compared with other reactive lymphadenopathy or extranodal IgG4-related disease, suggests that there may be a relationship at least between nodal IgG4-related disease and EBV. It is important to avoid overdiagnosing these cases as malignant lymphomas or EBV-related lymphoproliferative disorders.

Key Words: IgG4-related lymphadenopathy, IgG4-related disease, Epstein-Barr virus

(*Am J Surg Pathol* 2014;00:000–000)

IgG4-related disease is a recently recognized systemic syndrome with unique clinicopathologic features, which frequently include lymphadenopathy.[1] Five histologic patterns are recognized in lymph nodes. The type with progressively transformed germinal centers (PTGCs) has distinct clinical and pathologic features.[2] Although PTGC-type IgG4-related lymphadenopathy is often localized in submandibular lymph nodes and usually asymptomatic, as we previously reported, it usually persists and relapses, and some cases can progress to involve extranodal sites and/or have systemic lymphadenopathy. In other cases, prominent interfollicular expansion with increased immunoblasts and vascular proliferation are observed, which can mimic malignant lymphoma, especially angioimmunoblastic T-cell lymphoma (AITL).[1] Increased forkhead box P3-positive (FOXP3$^+$) regulatory T cells (Tregs) are usually observed in IgG4-related disease. Although the pathogenesis of IgG4-related disease remains to be solved, cytokines produced by Treg and type 2 helper T cells (Th2) are considered to play an important role.[3]

Epstein-Barr virus (EBV) is a common human herpes virus that infects >90% of the adult human population. After primary infection at an early age, the virus persists in a small population of B cells for life. Immunocompetent hosts are asymptomatic, and their lymph nodes show few EBV-encoded RNA–positive (EBER$^+$) cells, whereas those

From the Departments of *Pathology; ‖Otolaryngology, Head and Neck Surgery, Okayama University Graduate School of Medicine, Dentistry, and Pharmaceutical Sciences, Okayama; ‡Center for Antibody and Vaccine, Research Hospital, The Institute of Medical Science, The University of Tokyo, Tokyo; §Department of Pathology, Okazaki City Hospital, Okazaki; ¶Department of Otolaryngology, Himeji Red Cross Hospital, Himeji; †Department of Diagnostic Pathology, Kobe University Graduate School of Medicine, Kobe; Departments of #Clinical Laboratory; **Pathology and Laboratory Medicine, Nagoya University Hospital, Nagoya, Japan; and ††Department of Pathology, Division of Hematopathology, University of Pittsburgh School of Medicine, Pittsburgh, PA.

M.T. and Y.S. contributed equally.

Conflicts of Interest and Source of Funding: The authors have disclosed that they have no significant relationships with, or financial interest in, any commercial companies pertaining to this article.

Correspondence: Yasuharu Sato, MD, Department of Pathology, Okayama University Graduate School of Medicine, Dentistry, and Pharmaceutical Sciences, 2-5-1, Shikata-cho, Kita-ku, Okayama 700-8558, Japan (e-mail: satou-y@cc.okayama-u.ac.jp).